University of Alberta

Changes in collateral blood flow and neuroprotective efficacy of transient aortic occlusion during acute ischemic stroke

by

Gomathi Ramakrishnan

A thesis submitted to the Faculty of Graduate Studies and Research
in partial fulfillment of the requirements for the degree of

Master of Science

Centre for Neuroscience

Spring 2014

Edmonton, Alberta

Dedication:

I owe my thanks to many individuals who helped and supported me throughout my masters program in Canada. First and foremost I would like to extend my sincerest thanks and appreciation to my principal investigator Dr. Ian Winship and other committee members Dr.Kathryn Todd, Dr. Fred Colbourne and Dr. Ashfaq Shuaib. Their constant motivation and nurturing has enabled me to adapt and prosper in my professional life and essentially made me a better person in life. I'm also glad that I got a wonderful opportunity to work with all of them. I would also like to thank my friend Bin Dong who helped me with my research. I would also like to extend my thanks to Sam Joshva, Shakib Rahman and other colleagues at the NRU for being supportive co-workers and also for providing a friendly environment conducive for scientific research. I would also like to thank some of my friends Greeshma, Divya and Sunantha for cheering me throughout the process. I would also like to express my gratitude to my family Ramakrishnan, Kamakshi and Meenu for their endless love, affection and understanding which gave me the confidence to come abroad to complete my masters programme. Last by not the least, I would like to extend a special thanks to my husband Prashanth for his unending support and belief which helped me to complete the program.

Abstract:

Ischemic stroke is the rapid loss of brain function due to occlusion of a cerebral blood vessel. It is a major cause of death and disability in the world; however, the approved thrombolytic treatments are ineffective in many patients and there is a need for better therapies for treating brain ischemia. One potential approach to enhance the cerebral perfusion to ischemic brain tissue is to augment collateral circulation. Collateral vasculature provides an alternate route for blood to reach ischemic tissue when the principal conduits are blocked. Collateral circulation can be augmented by transiently occluding the aorta to increase the cerebral blood flow. We investigated the efficacy of using transient aortic occlusion (TAO) in different models of ischemic stroke. Our findings suggest that TAO can augment collateral flow, though its efficacy varies in different models of stroke.

TABLE OF CONTENTS

LIST OF TABLES

LIST OF FIGURES

LIST OF ABBREVIATIONS

A	anterior
ACA	anterior cerebral artery
ANOVA	analysis of variance
ATP	adenosine triphosphate
BBB	blood brain barrier
CCA	common carotid artery
CCAo	common carotid artery occlusion
CT	computed tomography
CTA	computed tomography angiography
Dd	double distilled
ECA	external carotid artery
FGF	fibroblast growth factor
G-CSF	granulocyte colony stimulating growth factor
H&E	hematoxylin and eosin
HGF	hepatocyte growth factor
ICA	internal carotid artery
ICAo	internal carotid artery occlusion
ICH	intracerebral hemorrhage
L	lateral
LA	left anterior
LMA	leptomeningeal artery
LP	left posterior
LSCI	laser speckle contrast imaging

M	medial
MAP	mean arterial pressure
MCA	middle cerebral artery
MCAo	middle cerebral artery occlusion
MR	magnetic resonance
MRA	magnetic resonance angiography
NIHSS	national institute of health stroke scale
P	posterior
PCA	posterior cerebral artery
RA	right anterior
ROS	reactive oxygen species
ROI	region of interest
RP	right posterior
rt-PA	recombinant tissue plasminogen activator
SAH	subarachnoid hemorrhage
SD	standard deviation
SEM	standard error of mean
SPG	sphenopalatine ganglion
TAO	transient aortic occlusion
TCD	transcranial doppler ultrasonography
t-PA	tissue plasminogen activator
TPLSM	two photon laser scanning microscopy
VEGF	vascular endothelial growth factor
VEGFR	vascular endothelial growth factor receptor
WHO	world health organization

WKY	wistar kyoto rats

Σ	standard deviation
^{o}C	degree Celsius
Cm	Centimetres
G	Grams
Hr	Hours
I	mean intensity
K	speckle contrast factor
L	Length
μ	Viscosity
μm	Micrometer
Ml	Millilitre
mM	Millimolar
Q	Flowrate
R	Radius
R_h	hydraulic resistance
V	Velocity
τ_c	correlation time

$CaCl_2$	calcium chloride
H_2O	Water
KCl	potassium chloride

$MgCl_2$	magnesium chloride
NaCl	sodium chloride
NH_3	Ammonia
NO	nitric oxide
N_2O	nitrous oxide
O_2	Oxygen

CHAPTER 1

Introduction

1.1. Stroke

Stroke is the rapid loss of brain function that results from the disruption of blood supply to the brain. It ranks as the third leading cause of death in Canada after heart disease and cancer.[1, 2] The annual cost for treating a disabled stroke patient in Canada is $107,883 and for treating a non-disabled patient is $48,339. Overall, stroke costs the Canadian economy 2.8 billion dollars every year. [3] Stroke risk is determined by a number of modifiable and non modifiable risk factors. Modifiable risk factors for stroke includes hypertension, cardiac morbidity, cigarette smoking, diabetes, high levels of alcohol consumption, high cholesterol levels and high homocysteine levels, [4] while age is the primary non modifiable risk factor of stroke. [5]

Stroke can affect the whole brain or a particular region of the brain. The former is termed as a global stroke while the later is referred to as a focal stroke. A focal stroke can be hemorrhagic or ischemic. Hemorrhagic stroke accounts for 5 to 15% of all strokes [6] and is caused by the bleeding of cerebral blood vessel in or around the brain. Hemorrhagic stroke can be classified into two sub groups; intracerebral hemorrhage (ICH) and subarachnoid hemorrhage (SAH). ICH involves bursting of a blood vessel within the brain while SAH involves rupture of a blood vessel within subarachnoid space. ICH and SAH have mortality rates ranging from 35% -

52% and 33% - 45% at 30 days from stroke onset respectively. [7, 8] Although hemorrhagic stroke has a higher mortality rate than ischemic stroke, it is less common. Ischemic stroke accounts for 87% of all strokes. [9] An ischemic stroke is caused by the blockage of a cerebral blood vessel. Ischemic stroke is differentiated from transient ischemic attacks (TIA) by neurological symptom that lasts longer than 24 hours and has a mortality rate of 25% after 30 days from stroke onset. [10, 11,12] Mortality rate or the extent of disability in survivors due to an ischemic stroke is governed by the location of an occlusion and its corresponding infarct size.

Brain injury after an ischemic stroke occurs due to pathophysiological mechanisms such as excitotoxicity, peri-infarct depolarization, and inflammation that lead to cell death that progress over space and time.[13] Irreversible tissue damage occurs in the ischemic core where the blood flow drops below 20% of the baseline perfusion.[11] The region around the ischemic core, the ischemic penumbra, has a partial maintenance of blood flow and the tissue damage here is reversible during the early stages of stroke.[14] Without treatment, the penumbra has the potential to grow into an infarct but the salvageable nature of this tissue is currently being investigated for “neuroprotective” treatments of ischemic stroke.

Numerous neuroprotective agents that have demonstrated efficacy in

preclinical trials have later been shown ineffective in clinical trials.[15, 16] In fact, tissue plasminogen activator (tPA) is the only drug proven to show a clinical benefit by reducing mortality and morbidity after an ischemic stroke. [17] However, tPA is limited by a short therapeutic window requiring administration within 4.5 hours of stroke onset[18]. Increasing the treatment window beyond this span increases the risk of hemorrhagic transformation from 6.4% to 21.2%,[19, 20] which has a devastating impact on recovery. [21] Meeting the criteria to receive tPA is therefore difficult due to the delays associated with stroke recognition, transport, triaging and neuroimaging, [22] and a study of ischemic stroke patients suggested that the tPA administration rates in the United States were as low as 2.40% in 2006. [23] Moreover, revascularization rates for acute ischemic stroke patients with tPA treatment may be as low as 6% for internal carotid artery (ICA) terminus, 30% for middle cerebral artery (MCA) trunk occlusions and 30% for basilar occlusions. [24, 25] The limitations of tPA necessitate the development of new approaches for the treatment of ischemic stroke.

1.2. Cerebral Circulation and Circle of Willis

One neuroprotective approach to treat focal ischemic stroke is to increase the cerebral blood flow to the ischemic brain tissue through cerebral collateral circulation. Collaterals refer to the pre-existing network of blood vessels that direct cerebral blood flow to ischemic tissue during a major

cerebro vascular trauma. [26] Cerebral collaterals can be classified as primary and secondary collaterals. Primary collaterals include the collaterals of the Circle of Willis while the secondary collaterals include the ophthalmic collaterals and leptomeningeal collaterals. [26]

The Circle of Willis is the cerebral arterial circle at the base of the brain that creates redundancy in cerebral blood flow between the internal carotid arteries and vertebrobasilar system.[27] During occlusion or stenosis, Circle of Willis reroutes and maintains blood flow in regions downstream of narrowing or occlusion.[28] The anterior cerebral artery (ACA), anterior communicating arteries, internal carotid artery, posterior cerebral artery (PCA), and posterior communicating artery constitute the Circle of Willis, while the basilar artery and middle cerebral arteries are connected to the Circle but not considered as constituent vessels. [29]

Functionally, ACA and its branches supply the medial and dorsal part of the cortex. The MCA supplies the lateral surface of the cortex, sub cortex, thalamus, basal ganglia and deep structures in the lateral cerebrum. The PCA, which curves around the brainstem supplies the ventral and posterior surfaces of the cortex.[29] These major cerebral arteries branch into progressively smaller arteries and surface arterioles. The surface arterioles gives rise to penetrating arterioles, which penetrate into the brain tissue.

Penetrating arterioles gives rise to parenchymal arterioles that supply the capillaries in the microvascular bed. The regulation of flow in capillaries is dependent on the regulation of flow and microvascular pressure in the arterioles. [30] These capillaries drain into venules and then into larger veins. The cortical veins empty into superior sagittal sinus while deep veins empty into superior sagittal sinus, inferior sagittal sinus or great vein of Galen. Venous flow is then directed towards torcular Herophili (confluence of sinuses) and then on toward central circulation via transverse sinus, sigmoid sinus and jugular veins. [30]

1.2.1. Secondary collaterals in the brain

As mentioned earlier, ophthalmic collaterals and leptomeningeal collaterals are the secondary collaterals in the brain. Like primary collaterals, the ophthalmic collaterals can also partially restore blood flow to the distal carotids during internal carotid artery occlusion or stenosis. [31, 32] The leptomeningeal collaterals or pial collaterals allow blood flow through anastomoses between the distal branches of the cerebral arteries found on the surface of the brain thereby permitting flow into the territory of the obstructed artery.[33] Since this thesis focuses on role of leptomeningeal collaterals after cerebral ischemia assessed via in vivo imaging, the methods to image cerebral collateral blood flow will be discussed briefly below.

1.3. Imaging collateral circulation

This section will briefly outline some of the techniques used for imaging collateral blood flow in humans and animal studies. Since collateral circulation is an important predictor of infarct size,[34, 35, 36] it is essential to have an accurate imaging modality to optimize its predictive value and to properly evaluate the benefits and mechanisms of collateral therapeutics.

1.3.1. Collateral blood flow imaging in humans

Cerebral blood flow can be imaged using a number of direct and indirect methods. Techniques such as magnetic resonance (MR) perfusion imaging, computed tomography (CT) perfusion, xenon-enhanced CT, single photon emission CT and positron-enhanced tomography can be used to indirectly measure cerebral perfusion during stroke, and make inferences on the collateral perfusion of ischemic tissue.[26] These methods have limited benefits since they offer only indirect information about the collateral perfusion.[26] Direct methods of measuring cerebral blood flow involve single vessel resolution and permit direct assessment of collateral blood flow in stroke patients.[26] Direct methods include cerebral digital angiography, magnetic resonance angiography, computed tomography angiography and transcranial doppler ultrasonography (TCD) and will be briefly discussed below.

Cerebral digital angiography involves injecting a contrast dye via the femoral artery during X-ray imaging. The series of radiographs collected during transfusion of contrast agent yields high resolution images of cerebral blood flow.[37]

Magnetic resonance angiography (MRA) maps the cerebral blood vessels using magnetic resonance imaging approach.[38] MRA is considered less toxic than conventional angiography since it does not use ionizing radiation or an invasive catheter. Though MRA techniques are considered as the most powerful non-invasive methods to examine collateral circulation and anatomical variations in Circle of Willis,[39] they cannot be used in patients with pacemakers or other magnetic appliances.[40]

Computed tomography angiography (CTA) is the most commonly used diagnostic vascular imaging tool in stroke patients.[41] It requires intravenous injection of iodine which permits fast acquisition of high resolution CT images of cerebral vasculature. CTA can effectively detect proximal arterial occlusion and predict functional outcome and response to thrombolysis. [37] Though CTA results in fewer motion artefacts, the risk of radio-contrast nephropathy after CTA is a major concern especially in patients with kidney disease or diabetes.[40]

TCD uses spectral Doppler sampling over specific cerebral blood vessels to measure the blood flow velocity within the vessel. Though TCD provides real time information on cerebral blood flow without exposing patients to radiation, it does not allow 2D or 3D reconstruction of vascular networks in the brain.[40,37]

1.3.2. Collateral blood flow imaging in laboratory animals

Imaging collateral blood flow in animal models of stroke provides an opportunity to study the importance of collateral circulation, collateral dynamics during stroke and the efficacy of collateral therapeutics as a treatment for stroke. The methods for imaging single vessel blood flow in animal models of stroke include two photon laser scanning microscopy (TPLSM) and laser speckle contrast imaging (LSCI), which will be discussed briefly below.

TPLSM is a technique that allows visualization of cerebral blood vessels up to 1mm below the surface of the brain. TPLSM uses longer excitation wavelengths that have lower photo-toxicity and it allows for optical sectioning and 3D reconstructions of blood vessels.

TPLSM accurately measures cortical microcirculation after labelling blood plasma with fluorescent conjugated dextran. This technique allows very

high resolution of blood flow in arteries and veins on the surface of the brain in addition to arterioles, venules and capillaries in the micro vascular bed below the brain surface. Moreover, it allows for precise quantification of direction and velocity of red blood cells within the vessel.[37] An example of imaging blood vessels using TPLSM is given in Figure 1.

In addition to imaging cerebral blood vessels, TPLSM can also be used to study dendritic microstructure of individual neurons[42,43] and also allows calcium imaging in mice during acute ischemic stroke.[44, 45]

While TPLSM gives an accurate blood flow measures, it is an expensive technique requiring rare instrumentation. LSCI, however, requires only inexpensive and readily available instrumentation and is extremely useful in mapping collateral blood flow changes on the surface vasculature of the brain. LSCI provides high-resolution maps of blood flow on the cortical surface of the brain. [46] Preparations and data acquisition and analysis for this technique are described in detail in the methods section to follow and data acquired using LSCI are illustrated in Figures 2 and 3.

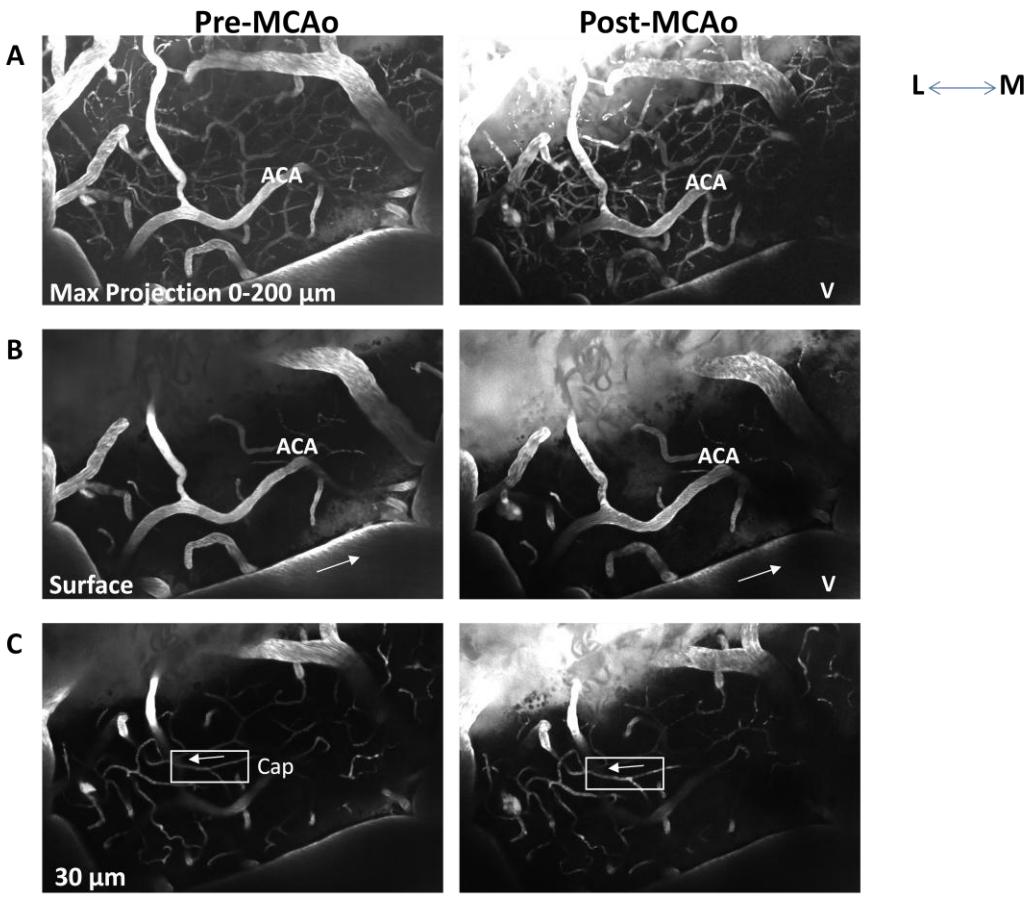

Figure 1. Blood flow imaging using two photon laser scanning microscopy (TPLSM). TPLSM imaging showing cerebral blood flow maps in ACA territory before and after MCAo. Arrows denote directions of blood flow in a branch of the ACA and adjacent surface vein (V). (A) The top row shows a maximum projection through all images in the first 200 microns below the surface vasculature in the territory of ACA before and after MCAo. (B) The middle row below shows projections from 2-4 image planes centered at 30 microns below the surface. (C) The last row below shows projections from 2-4 image planes centered at 80 below the surface.

1.4. Leptomeningeal collaterals

As noted previously, a leptomeningeal artery (LMA) is a pial artery that connects two major cerebral arteries that provide blood flow to different areas of cerebral cortex. [47] The direction of blood flow through a LMA is influenced by pressure drop between the ends of the joined arterial segments. The compensatory capacity of one LMA is inversely related to its hydraulic resistance, which is a measure of its opposition to the passage of fluid flow [48] and is given by the following equation for a blood vessel of circular cross section.[47]

$$R_h = \frac{8\mu L}{\pi R^4}$$

Where R_h is the hydraulic resistance, μ is the viscosity of the flowing fluid, L is the total length of the vessel and R is the radius of the vessel. From this equation it can be interpreted that the compensatory capacity of a LMA is directly proportional to the fourth power of its radius and changes in dilation of an artery would have a very high impact on its compensatory capacity. A large number of clinical and pre clinical studies support the existence and importance of LMA in stroke.

1.4.1. Leptomeningeal collaterals in clinical settings

Clinical studies have shown that leptomeningeal collaterals are linked to positive outcomes after stroke by reducing infarction volumes and

improving functional recovery. [49, 50,51] However, while leptomeningeal collaterals are observed as a positive indicator of post stroke outcome, in some cases the presence of leptomeningeal collaterals in humans can signify the presence of cerebrovascular impairment such as vascular occlusive disease that might predict stroke in some individuals.[37] For example, Moyamoya disease is a progressive cerebrovascular disorder leading to transient ischemic attacks, strokes, headaches and seizures. The angiographic features of this disorder are progressive stenosis or occlusion of internal carotid artery (ICA) accompanied by occlusion of parenchymal (Moyamoya), transdural and leptomeningeal collaterals.[52] This chronic occlusion results in highly developed leptomeningeal arteries which are a positive indicator of ischemic symptoms [53] and are associated with puffy pial networks and slow cerebral perfusion.[54] Yamuchi et al [55] demonstrated that the patients with well developed ophthalmic or leptomeningeal collaterals during an ICA occlusion often suffer from chronic cerebrovascular impairment.

In patients without cerebrovascular impairment, collateralization is associated with better outcomes after stroke. Christoforidis et al [49] showed that ischemic patients with better angiographically assessed collateral scores have smaller infarction volumes and lower modified Rankin scale scores at discharge. The same study also found that the patients with lower

collateral scores had significantly higher NIHSS scores accounting for their poor functional recovery. Patients with good collateral grades also have better recanalization rates after endovascular recanalization therapy.[35,56] Lima et al [51] found that patients with a favourable pattern of leptomeningeal collaterals along with younger age, lower baseline NIHSS, absence of diabetes and administration of rtPA predicted improved outcome at 6 months after stroke. Additionally, Christoforidis et al [52] demonstrated that poor leptomeningeal collateral circulation in patients was associated with higher incidence and larger size of hemorrhagic transformation after intra-arterial thrombolysis. The rates of significant hemorrhage were 25% in patients with poor leptomeningeal collaterals and 2.78% in patients with good leptomeningeal collaterals. Additionally, good collateral status might improve the efficacy of thrombolytic drug therapies such as rtPA by increasing the routes for these pharmacological agents to reach the clot, thus aiding recanalization.[37]

1.4.2. Leptomeningeal collaterals in pre-clinical settings

While evaluating collateral dynamics and therapeutics in animal models, it is important to consider variation of native collaterals in different strains. [37] The density and diameter variation of these native collaterals in C57BL/6 and BALB/c mouse strains are accompanied by large difference in infarction volume after an occlusion.[57] Zhang et al, [36] showed that the

extent of the native pial collateral circulation and collateral remodelling after MCAo vary widely with genetic background, and the infarction volume correlated inversely with collateral number, diameter and number of penetrating arterioles in 16 different mouse strains.

Early pre-clinical studies focussed on the regulation of leptomeningeal collateral blood flow. Menzies et al, [58] showed that the pyriform branch of MCA collaterallizes with ACA and the parietal and temporal branches of MCA have collateral communication with posterior cerebral artery after MCAo in Sprague-Dawley rats. In the case of MCA occlusions (MCAo), blood flow through the leptomeningeal anastomoses arrives from the arterial branches of the anterior cerebral artery (ACA) and posterior cerebral artery (PCA).[58] A study using laser Doppler flowmetry in SD rats suggests that pial arteries takes around 12 seconds to become maximally dilated and around 131 seconds to become stable after a common carotid artery occlusion (CCAo). [59] This dilation of pial artery after MCAo or CCAo increases cerebral perfusion after stroke. [59,60] However, while leptomeningeal arteries increase cerebral blood flow, they do not provide enough blood flow to maintain normal cerebral perfusion over a long time period. [61]

A study using laser speckle contrast imaging (LSCI) shows that 75% of

MCA-ACA anastomoses formed after a MCAo in Sprague Dawley (SD) rats last for 24 hours post stroke. Though the amount of blood flow through these MCA-ACA anastomoses was not quantified, this data suggests they can provide immediate and persistent blood flow to the ischemic territories, at least during the first 24 hours after stroke. [46]

Changes in leptomeningeal collaterals are also observed during long term recovery from MCAo. Coyle and Heistad [62] showed that leptomeningeal collaterals supplying blood to MCA territory were able to restore blood flow to near baseline levels in that territory one month after MCAo in normotensive Wistar Kyoto (WKY) rats. They exhibited extreme collateralization (~27 anastomoses between MCA and ACA) and small infarct at one month after chronic MCAo. In contrast, stroke prone hypertensive rats also exhibited extreme collateralization, although their anastomoses were significantly narrower than normotensive WKY rats and hypertensive rats had a larger infarction at 1 month after MCAo.[62]

1.5. Collateral blood flow augmentation

Cerebral collateral circulation can be augmented by various treatments including angiogenesis, mild induced hypertension, sphenopalatine ganglion stimulation, head positioning and transient aortic occlusion. Augmenting collateral blood flow might maintain blood flow in the ischemic penumbra

and thereby reduce cell death in this at-risk tissue. However, collateral therapeutics remains a mostly unexploited neuroprotective strategy. [37]

1.5.1. Collateral angiogenesis

Angiogenesis is mediated by a number of angiogenic factors including vascular endothelial growth factor (VEGF), fibroblast growth factor (FGF), granulocyte colony stimulating growth factor (G-CSF) and angiopoietin and can be induced by recruitment of circulating inflammatory cells to the site of angiogenesis. [63, 64]

For example, an intra-cerebroventricular injection of VEGF using an osmotic pump starting 24 hours after the onset of focal cerebral ischemia in a rodent model of stroke stimulated angiogenesis that coincided with a reduction of infarction volume.[65] Similarly, increased angiogenesis by late administration (48 hours after the onset of ischemia) of VEGF was associated with reduced neurological deficits in a rat model of embolic stroke.[66] However, apart from having a critical role in angiogenesis, VEGF also functions as a vascular permeability factor, which might result in BBB breakdown, edema, vasodilation and abnormal system hemodynamics.[67] Furthermore, the neuroprotective dosage of VEGF is different from the dosage of VEGF required to instigate angiogenesis and the angiogenic dosage of VEGF might be neurotoxic.[68] Further studies in stroke recovery

are required to determine the optimal balance between the neuroprotection offered by VEGF through angiogenesis and neurotoxicity of VEGF through BBB breakdown.[69]

Hepatocyte growth factor (HGF) is another angiogenic growth factor which enhances the growth of endothelial cells. HGF has been shown to improve the blood flow by increasing the number of collateral vessels after hindlimb ischemia in rabbits.[70]

Other promising mediators of angiogenesis are G-CSF and granulocyte monocyte colony stimulating factor (GM-CSF). A number of groups have identified the neuroprotection offered by G-CSF and GM-CSF before or after ischemia in rodent models.[71,72,73] Sugiyama et al [74] demonstrated that five days of daily administration of G-CSF or GM-CSF after a unilateral occlusion of common carotid artery in C57/BL6 mice improved leptomeningeal collateral growth and decreased infarct volume. A subset of these animals subjected to MCAo, seven days after common carotid artery occlusion were treated with G-CSF or GM-CSF had greater cerebral perfusion and smaller infarction volume than untreated animals.

Although angiogenic factors offer a promising therapy for ischemic stroke in animals further research are warranted for it to proceed to clinical

research.

1.5.2. Mild induced hypertension

Pharmacological agents such as phenylephrine, or angiotensin can be used to induce mild hypertension, which increases global cerebral blood flow and may therefore promote blood flow through leptomeningeal collaterals to the salvageable penumbra.[75, 76] Animal models have confirmed the neuroprotection offered by mild induced hypertension. An increase in cerebral blood flow and decrease in lesion volume was observed in rats and rabbits when phenylephrine was used to induce mild hypertension as early as one hour after MCAo.[77, 78] Similarly angiotensin also demonstrated an increase in mean arterial pressure and reduction in infarction volume after transient MCAo in rats.[79] While mild induced hypertension might be neuroprotective, it is important to note that this treatment might increase the risk of intracerebral hemorrhage, reflex bradycardia and ischemic bowel disease.[75]

In clinical trials, the elevation of systemic blood pressure after stroke has not demonstrated unequivocal beneficial results in long-term neurological outcome.[26] However, some studies show that inducing mild hypertension can improve functional outcome measured by NIHSS scores and volume of hypoperfused tissue. [80,81] There is a need for future trials on mild induced

hypertension which might provide an alternate for patients who are ineligible for thrombolysis.

1.5.3. Sphenopalatine ganglion stimulation

Another approach to augment cerebral circulation is to manipulate neurovascular interface during stroke. Sphenopalatine ganglion (SPG) stimulation involves stimulating the parasympathetic fibres that innervate the anterior cerebral circulation and thereby evoking significant increases in cerebral blood flow.[82,83,84] Recently, SPG stimulation in rats showed an increase in cerebral blood flow with vasodilation of cortical arterioles and a reduction in BBB dysfunction and stroke volume. This therapeutic effect was observed even when SPG stimulation was applied 24 hours after stroke onset.[85] In addition to improving blood flow to the brain, SPG stimulation has also shown to improve functional recovery at 8 and 28 days after stroke in rats even when applied 18 hours after stroke onset. [86] Pre-clinical data suggests that SPG stimulation might extend the therapeutic window of stroke. Clinical trials are currently evaluating the safety of SPG stimulation's use in ischemic stroke patients. [87]

1.5.4. Head positioning

Cerebral blood flow may also be augmented by supine positioning of the head that increases arterial blood flow due to gravity. Notably, this

treatment can be offered as soon as an ischemic stroke is diagnosed. Preliminary data from twenty patients suggests an increase in blood flow velocity of 20% in the middle cerebral artery (MCA) after a head positioning of 30º to 0º elevation during the first 24 hours after ischemic onset, resulting in functional improvement.[88] Conversely, a decrease in cerebral blood flow was observed when the head elevation was changed from 0º to 30º or 45º. [89, 90] Even though supine head positioning increases blood flow, it should be noted that it might increase the intracranial pressure of some patients, whereas elevating the head promotes a reduction in intracranial pressure. Therefore it is advisable to determine optimal head positioning for patients individually rather than routinely establishing a head position. [89] More research is required on head positioning since it is unclear of what extent it can alter the collateral blood flow and also how the delay and duration of supine positioning can affect the outcome.

1.5.5. Transient aortic occlusion

Transient aortic occlusion (TAO) attempts to increase cerebral blood flow by partially occluding the descending aorta. In TAO, a catheter is inserted via femoral artery and inflated to occlude 70% of the descending aorta thus increasing global cerebral circulation and perfusion of ischemic territories by collateral pathways.[37] Initially, TAO was used to treat symptomatic vasospasm after subarachnoid hemorrhage, where it showed the potential to

improve cerebral perfusion and neurological outcome.[91] TAO in a non ischemic porcine model increases cerebral blood flow by 35-52% , even 90 minutes after removing the catheter.[92] Additionally, TAO after a thromboembolic stroke in SD rats significantly reduced the infarction volume at 24 hours after MCAo, without increasing the risk of hemorrhagic transformation. The infarction volume was further reduced when the treatment was combined with rtPA.[93]

Pre-clinical work in our lab supports a role for TAO collateral blood flow augmentation. Twenty male Sprague Dawley rats (400-550 g) were randomly assigned to one of the four following groups. (1) Sham stroke+ Sham TAO (2) Sham stroke+ TAO (3) Stroke+ sham TAO (4) Stroke+TAO. Laser speckle contrast imaging (LSCI) was used to map the collateral blood flow changes in the distal branches of MCA and to measure the relative changes in blood flow on this surface vasculature.

Briefly, SD rats were anesthetized and implanted with a chronic thin window followed by baseline blood flow imaging.[94] The rats were subjected to MCAo by thromboembolic model and the collateral blood flow through the MCA-ACA anastomoses was then imaged using LSCI. Sham or TAO was induced after post- stroke imaging for 45 minutes and LSCI blood flow maps were collected at the end of the 45 minutes of sham/TAO

(with catheter still in place). Lighter LSCI maps reveal lower blood flow and darker LSCI maps reveal higher blood flow. LSCI maps from Sham stroke + Sham TAO, Sham stroke + TAO, Stroke + TAO and Stroke + sham TAO, groups are given in Figure 2A, 2B, 3A and 3B respectively.[95,96]

As shown in Figure 2, the maps of blood flow attained via LSCI in sham-MCAo animals were highly consistent over imaging sessions, irrespective of TAO or sham-treatment. [95,96] Importantly, these animals did not exhibit anastomotic connections between the distal segments of the ACA and MCA. Conversely, MCAo induced clear changes in blood flow downstream of the occlusion (Figure 3). [95,96] Immediately after MCAo, robust anastomotic connections between distal segments of the ACA and MCA (Figure 3, arrows in middle panels) were observed in all animals. These leptomeningeal anastomoses remained stable during post-MCAo imaging sessions in sham- and TAO-treated animals, as all ACA-MCA anastomoses identified immediately post-MCAo persisted until the final imaging session 45 minutes after treatment. [95,96]

Preliminary analysis of the LSCI images was performed to obtain the speckle contrast factor (K), which is a measure of the local spatial contrast of the laser speckle pattern. K values are inversely related to the blood flow and it ranges from 0 to 1, with values near 1 suggesting no blood flow in

that vessel and values closer to zero reflect greater blood flow.[37] While LSCI reveals changes in pattern of blood flow, the exact quantitative relationship between K and blood flow velocity remains undefined.[97] Therefore, in this thesis, we have used these LSCI maps to determine more quantitative changes in blood flow due to TAO.

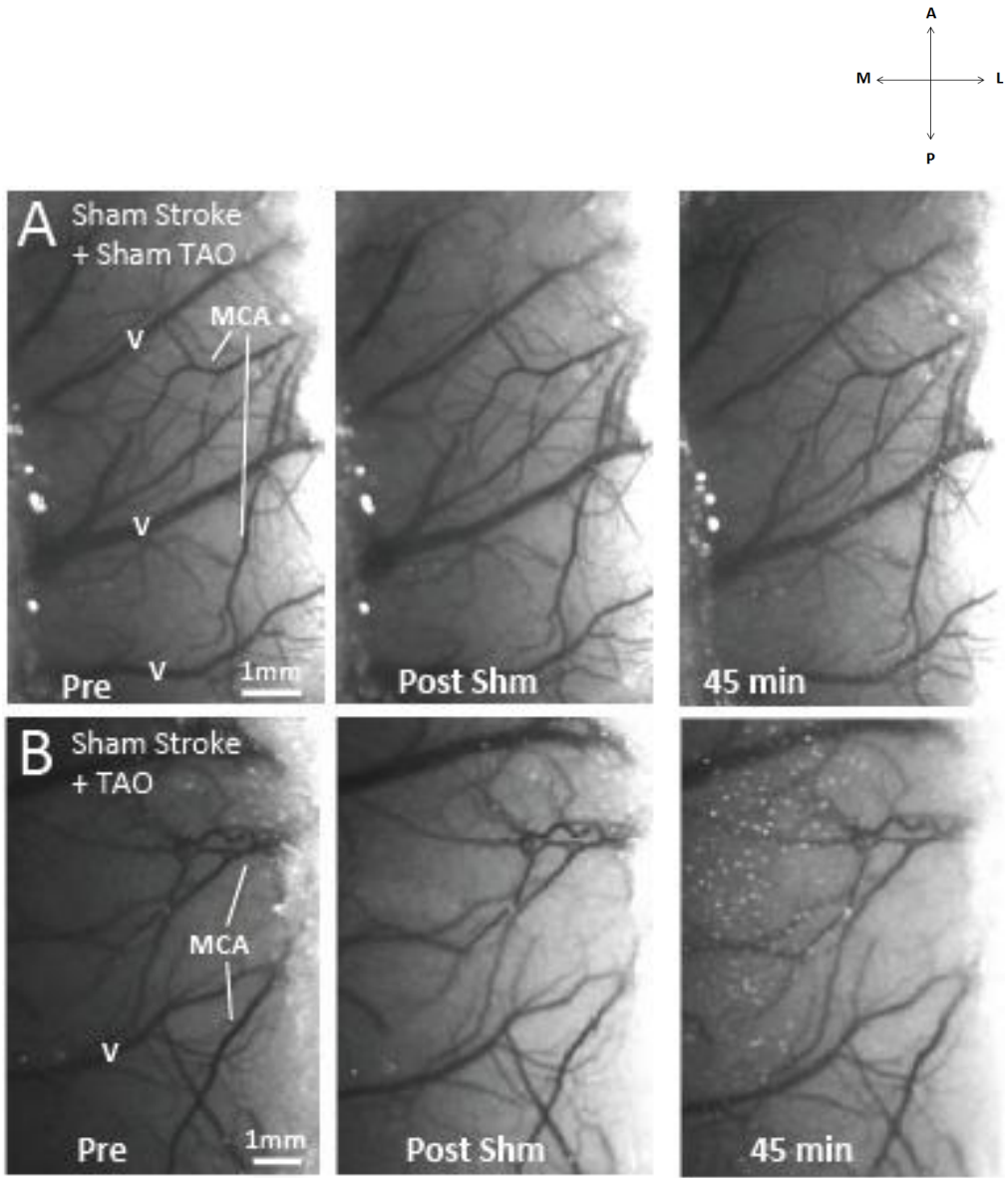

Figure 2. Mapping blood flow after sham stroke and during treatment using laser speckle contrast imaging (LSCI). LSCI imaging showing a map of single vessel blood flow in surface veins (V) and distal branches of MCA over the hindlimb and forelimb sensory motor cortex. (A) Left and the middle panels show blood flow before and after Sham MCAo mapped with LSCI, whereas the right panel shows blood flow during 45th minute of sham TAO treatment. (B) Left and the middle panels show blood flow before and after sham MCAo mapped with LSCI whereas the right panel shows blood flow during 45th minute of TAO treatment. A, Anterior; P, Posterior; M, Medial; L, Lateral.[95 ,96]

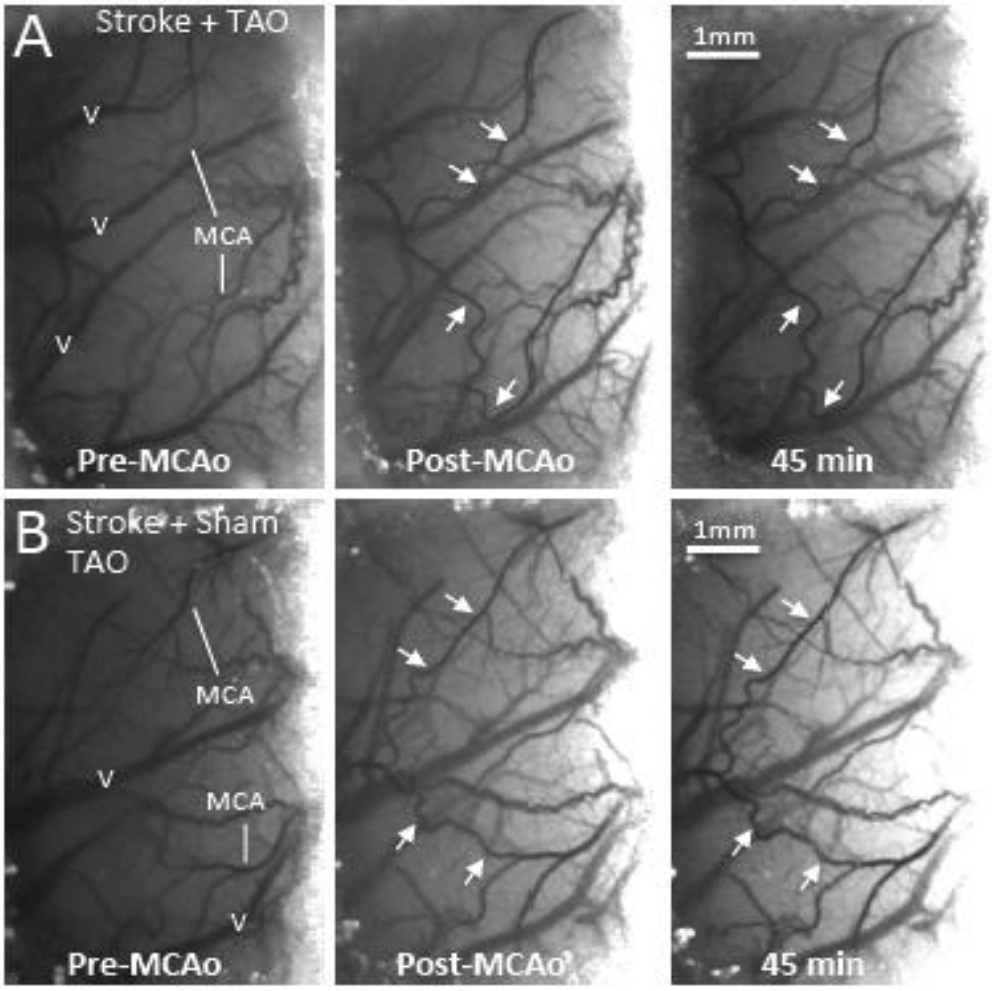

Figure 3. Mapping blood flow after focal ischemic stroke and during treatment using laser speckle contrast imaging (LSCI).LSCI map showing blood flow in surface veins (V) and distal branches of MCA over the hindlimb and forelimb sensory motor cortex. Arrows indicate the blood flow through the anastomotic connections between the distal branches of MCA and ACA immediately after a MCAo.(A) Left and the middle panels show blood flow before and after MCAo mapped with LSCI, whereas the right panel shows blood flow during 45th minute of TAO treatment. Darker MCA branches are indicative of higher blood flow during TAO. (B) Left and the middle panels show blood flow before and after MCAo mapped with LSCI whereas the right panel shows blood flow during 45th minute of sham treatment. Lighter MCA branches are indicative of slower blood flow during sham treatment.[95 ,96]

Clinically, the safety profile of TAO was recently tested on patients up to 14 hours after stroke onset and confirmed that TAO is safe with no increase in adverse events when compared to the standard treatments.[98] Although the efficacy of TAO in this study remained unclear, TAO was suggested to be effective in patients when the treatment was given within 5 hours of stroke onset, older than 70 years of age and with moderate stroke severity.[98] This trial did not show a clear clinical benefit, possibly due to including patients who did not have a viable penumbral tissue. Future trials on selected patients with persisting penumbral tissue might show a better efficacy after TAO intervention. [99] Moreover, TAO as an adjunct to thrombolysis in the treatment of acute ischemic stroke appears safe and future studies on TAO are warranted. [100] Recently, data suggests TAO may be a therapeutic option for patients who do not show improvement with rt-PA treatment with by improving blood flow during the procedure. [101]

1.6. Research aims

As mentioned above, collateral circulation can be augmented to increase cerebral blood flow. In particular, TAO may improve the cerebral perfusion after a moderate MCAo. However, little is known about the mechanisms, efficacy and extent of neuroprotection offered by TAO after an ischemic

stroke. The studies described in this thesis use LSCI for measuring the relative changes in blood flow at various time points. The aims of this thesis are as follows. (1) To more quantitatively illustrate changes in blood flow during TAO in previously acquired LSCI data (2) To demonstrate long term neuroprotection offered by TAO in thromboembolic model of MCAo (3) To evaluate persistent TAO induced blood flow changes in a large stroke model where the clot cannot shift.

CHAPTER 2

Materials and Methods

2.1. List of solutions

2.1.1. Eosin solution

To 3.96ml Eosin Y add, 30.9ml 95% ethanol, 158.2µl Glacial acetic acid.

2.1.2. 1% Ammonia water

Add 8ml of 25% NH_3 to 192ml ddH_2O.

2.1.3. Cresyl violet Solution A

Add 68g of Sodium acetate to 500ml of ddH_2O.

2.1.4. Cresyl violet Solution B

Add 60ml of glacial acetic acid to 940ml of ddH_2O.

2.1.5. Cresyl violet Solution

Add 5g of Cresyl violet to 600ml of ddH_2O. Then add 640ml of Cresyl violet Solution A and 340ml of cresyl violet Solution B to it.

2.1.6. Artificial cerebrospinal fluid

Dissolve 7.889 g NaCl, 0.4025g KCl, 0.204g $MgCl_2$-$6H_2O$,0.265 $CaCl_2$ and 1.3025g HEPES-Na into 1L dd H_2O. Adjust pH to 7.4 and vacuum filter with 0.02 micron filter.

2.1.7. 1.3% Agarose

Add 200mg of agarose to 15ml artificial cerebrospinal fluid. Then heat this solution until it boils and gradually cool it down to 37 ^oC before using it on the animal.

2.1.8. 20% Urethane

Add 20 g of urethane in 100ml of saline.

2. 2. Assessing cortical blood flow dynamics of TAO in rats

Experimental protocols conform the guidelines established by Canadian Council on Animal Care and were approved by the Health Sciences Animal Care and Use Committee at University of Alberta.

Briefly, animals were first anesthetized and implanted with a chronic thin window. Baseline blood flow maps were obtained using LSCI followed by MCAo and LSCI to measure the collateral blood flow through the MCA-ACA anastomoses. TAO was induced for 45 minutes as described below. The blood flow maps were acquired during TAO or acquired immediately after TAO and 1 hour after TAO. Throughout the surgery and imaging, rats were maintained at a temperature of 36.7 ^{o}C, and heart rate, oxygen saturation and breath rate were monitored using a MouseOx® pulse oximeter (STARR Life Sciences^{TM}).

2.2.1. Thin window placement

In brief rats were anesthetized with 1.5% isoflurane in a 30:70 mixture of O_2 and N_2O. A 5×5mm section of the skull was thinned over the right

sensorimotor cortex (approximately 1 to 5mm lateral to midline and -5mm from bregma as given in Figure 4.),[95, 102] using a dental drill. Artificial cerebrospinal fluid was often flushed over the window while thinning it to avoid the excess heat generation. The window was thinned until the vasculature was visible and then it was smoothed with a scalpel. A layer of 1.3% low melt agarose (in brain buffer) was then placed on the skull followed by sealing with a coverslip.

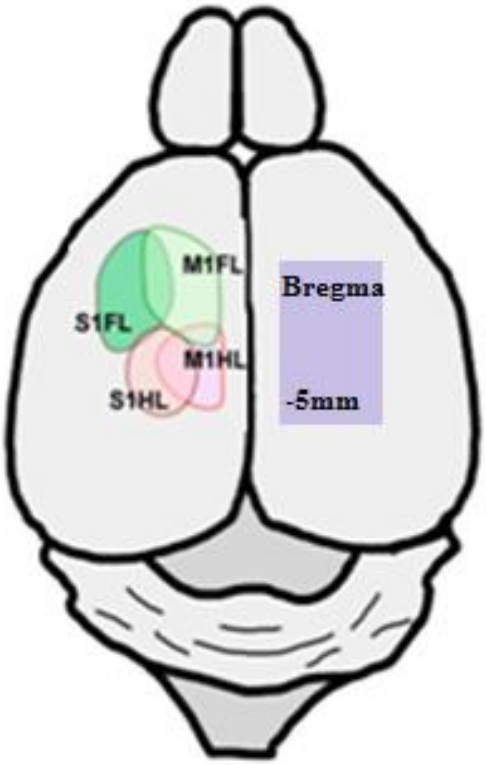

Figure 4. Thin window placement. The thin window was placed 1mm lateral to bregma and -5mm from bregma. This encloses the S1 FL- primary forelimb sensory motor cortex; S1HL-primary hindlimb sensory motor cortex; M1 FL- primary forelimb motor cortex; M1HL- primary hindlimb motor cortex. A coverslip was placed over the thinned window.[95]

2.2.2. Thromboembolic model of MCAo

Thromboembolic model of middle cerebral artery occlusion (MCAo) involves injecting an autologous blood clot through the ECA into the MCA and it closely resembles the thromboembolism that occurs in patients.[103] In this thesis, thromboembolic middle cerebral artery occlusion was induced as previously reported.[104] Anesthetized rats were placed in supine position and a longitudinal incision of 1.5cm was made on the ventral cervical skin. The right common carotid artery (CCA), right internal carotid artery (ICA) and right external carotid artery (ECA) were exposed. The distal portion of ECA was ligated and cut. Blood was withdrawn for clotting from ECA in a modified PE-10 catheter filled with bovine thrombin (From Jones Pharma incorporated). After the formation of blood clot (15 minutes), a PE-50 catheter was attached to 1.5cm of a PE-10 catheter and it was advanced for 17mm in the ICA until it reached the origin of MCA. The clot was then injected into the MCA, followed by catheter removal and closure of the wound.

2.2.3. Filament model of MCAo

Filament model of middle cerebral artery occlusion is a highly reproducible model which involves insertion of a silicon based filament to block blood flow at the junction of ACA and MCA.[103] In this experiment, filament model of MCAo was induced as previously reported.[105] Rats were

anesthetized by intraperitoneal injection of urethane at a dosage of 150mg urethane /100g body weight. Anesthetized rats were placed in a supine position and a longitudinal incision of 1.5cm is made on the ventral cervical skin. The right common carotid artery (CCA), right internal carotid artery (ICA) and right external carotid artery (ECA) are exposed. The distal portion of ECA was ligated and cut. A silicon based monofilament of 0.54mm diameter (Doccol Corporation) was advanced through the ICA and left in place when it reached the MCA. The filament was sutured in place and the wound was closed for before imaging procedure.

2.2.4. Transient aortic occlusion

The anesthetized rats were placed in supine position and a 2 cm long incision was made on the right hind limb skin. The femoral artery was extracted and 10cm of an uninflated catheter (2 mm diameter; Cordis fire star, RXPTCA dilation catheter) was inserted from the femoral artery up to the descending aortic arch. Then the catheter was inflated and rested in place for 45 minutes. The catheter was removed after 45 minutes and artery reconstruction was performed. The wound was sealed. In Sham TAO, rats were placed in supine position and the catheter was not inserted.

2.2.5. Laser speckle contrast imaging and analysis

Laser speckle contrast imaging (LSCI) was used to measure the relative changes in blood flow on the surface of the brain. It has been widely used in animal models for measuring cerebral blood flow changes after MCAo using thinned window or craniotomy preparation.[46, 77, 106, 107] In LSCI imaging, rats were placed in a custom made stereotaxic plate under a Dalsa 1M60 Pantera camera mounted on a video macroscope. 400 image frames are collected at 20 Hz (15 ms exposure time) during illumination with a 782nm Laser (Stocker Yale Inc.) on the lateral edge of the implanted window.

In the LSCI map, the number of MCA-ACA anastomoses that were formed after MCAo and the number of remaining anastomoses during treatment was counted and normalized to the corresponding length of the imaging window.

Laser speckle maps were analysed using Image J software (NIH). Laser speckle maps are based on the blurring of the laser speckle pattern by moving particles (such as blood cells). By measuring the changes in the speckle pattern the relative changes in the blood flow can be calculated. The speckle contrast factor (K) is a measure of the local spatial contrast of

the laser speckle pattern and is defined as the ratio of the standard deviation to the mean intensity ($K = \sigma s/I$) in a small region of the speckle image (typically 5× 5 or 7 x 7 pixels). *K* has a minimal value of 0 when the scattering particles are moving quickly, a maximal value of 1 with no movement, and is inversely related to blood flow velocity.[108, 109] By plotting K values, LSCI can reveal changes in the blood flow pattern after ischemia including enhanced collateral flow or reperfusion. To provide a better estimate of relative changes in blood flow velocity, speckle contrast values were converted to correlation times (τ_c) that are, in theory, inversely and linearly proportional to blood flow velocity (i.e. $1/\tau_c$ is proportional to the velocity of the blood flow at the ROI where speckle contrast was measured).[107] However, the assertion that correlation times are inversely proportional to blood flow is based on simplifying assumptions derived from literature using other imaging modalities and may not hold under all imaging and blood flow conditions.[109] We have therefore focused on within animal comparisons of changes in blood flow (as indicated by correlation times) as opposed to quantitative determinations of blood flow velocity.[96]

The relationship between speckle contrast, *K*, and τ_c is given by

$$K = \left[\frac{\tau_c}{2T}\left\{1 - exp\left(-2T/\tau_c\right)\right\}\right]^{\frac{1}{2}}$$

Where T is the exposure time of the camera (T=15ms in this thesis). $\tau_{Baseline}$ and τ_c are obtained using this equation. $\tau_{Baseline,}$ is the τ value obtained by substituting the value of $K_{Pre\text{-}MCAo}$ in this equation while τ_c is the τ value obtained by substituting "K" value of any imaging session in this equation. (During pre stroke imaging session; $\tau_{c=}\ \tau_{Baseline;}$ so, V=1).[96] Relative changes in blood flow velocity are calculated by using $\tau_{Baseline}$ and τ_c as given in the equation below.

$$V = \tau_{Baseline} / \tau_c$$

Where, V is the velocity of the liquid.

The changes in the blood vessel dilation were measured using a diameter plug in from Image J. This plug-in uses a full-width at half maximum algorithm to estimate the inner vessel diameter.[110] The diameter plug-in measures the diameter for five times in selected region of interest (ROI) in the loaded image. The diameter was measured at anatomically distinct regions of the arteries and the veins which is comparable across LSCI maps obtained during pre stroke, post stroke and sham/TAO imaging sessions. The volumetric flow rate through any blood vessel can be calculated through the given formula.

$$Q = \pi r^2 v$$

Where r is the mean radius of the vessel and v is the velocity of blood flow within a vessel.[96] When the value of v is substituted the equation becomes,

$$rel\ Q = \pi r^2(\tau_{Baseline} / \tau_c).$$

2.3. Histology

The brains obtained from the experiment were sectioned and stained as described in Sections 2.3.1 or 2.3.2 to confirm the presence of infarction. Lesion volume in these sections was analyzed as described below.

2.3.1. H and E staining

The frozen brain obtained from the experiment was sectioned into 20 micron thickness on the slides. They were stored in -20C until they were stained. Before staining, the slides were thawed to room temperature. The slides were immersed in Xylene for 2 minutes twice, followed by immersion in 100% ethanol, 90% ethanol, 2X ddH_2O for two minutes. Then they were immersed in filtered Harris Hematoxylin solution for 8 minutes followed by 3X ddH_2O wash. Next the slides were destained and differentiated by immersing in 0.5% hydrochloric acid in 70% ethanol for 2 seconds. This is immediately followed by a ddH_2O wash for 2 minutes. To increase the contrast of the stain the slides were immersed in 1% ammonia water for 25 seconds which was again followed by a 2X ddH_2O wash. Next the slides were immersed in Eosin solution for 7 seconds followed by 2X ddH_2O wash. Then the slides were washed in 90% and 100% ethanol consecutively for 1 minute twice. After which the slides were finally

immersed in Xylene before cover slipped with the Permount and allowed to dry overnight. Finally, the sides of the slides were closed with a colourless nail polish.

2.3.2. Cresyl Violet staining

The slides containing the sections were thawed to the room temperature. Then the slides were immersed in 70% ethanol solution for 5 minutes followed by immersion in 95% ethanol twice for 5 minutes per chamber. Then they were immersed in 100% ethanol twice for 5 minutes per chamber. After dehydration the slides were defatted by immersing them into Xylene for 5 minutes per chamber. Next the slides were immersed in 100% ethanol twice for 5 minutes per chamber followed by 95% ethanol wash twice for 5 minutes per chamber. This was followed by a 70% ethanol wash for 5 minutes. After which the slides are rehydrated and washed by ddH_2O twice. Then they were immersed in 1% cresyl violet solution for 5 minutes which is followed by ddH_2O wash for 5 times. Next the slides are immersed in 70% ethanol for 20 seconds followed by consecutive washes in 95% ethanol, 100% ethanol and Xylene twice for 5 minutes in each chamber. Then the slides are cover slipped with Permount and allowed to dry overnight.

2.3.3. Lesion volume analysis in experimental animals

The stained slides were scanned using Xerox work centre 5735 PS and images were saved in JPEG format. The lesioned areas in these images were selected using Image J software. Lesion volume was quantified based on the lesioned area, thickness of the sections and number of sections in between the lesion.

2.4. Statistical analyses

Statistical analysis and level of significance for anastomoses changes were confirmed by paired t-tests. Statistical analysis and level of significance for dilation of blood vessels, blood flow velocity and blood flow rate were confirmed by repeated measures ANOVA followed by post hoc comparisons which were restricted to within group comparisons using Tukey's HSD (where three or more groups were compared) and Sidak multiple comparisons tests (where two groups were compared).[96] The early and late lesion volume measurements were analyzed using t-tests while the changes in cortical and striatal infarction volumes were analysed by two way analysis of variance. Lesion volumes are expressed as Mean ± standard deviation (S.D). All other data are expressed as Mean ± standard error of the mean (SEM). Statistical significance was defined as $P < .05$.

CHAPTER 3

Results

3.1 Cortical blood flow dynamics during transient aortic occlusion in thromboembolic model of stroke

In this aim, previously acquired LSCI data was analyzed using more quantitative methods to better describe change in blood flow during TAO. The experimental outline for the imaging experiments in this objective is shown in Figure 5. The LSCI images for this experiment were acquired by Glenn Armitage and these images and his preliminary measures of speckle contrast are published as part of his thesis.[95] Twenty male Sprague Dawley rats (Size 400-550g) were used in this study. They were divided into four treatment groups (MCAo + TAO, MCAo + Sham TAO, Sham MCAo + Sham TAO, and Sham MCAo + TAO) prior to LSCI through a thin-skull imaging window. LSCI maps acquired from this experiment were further analyzed to determine the change in number of anastomoses after TAO in stroke induced rats, the correlation times for the blood vessels at different time points, the diameter of the blood vessels in the imaging window and blood flow rate within the blood vessels.[96] The brains obtained from this experiment were sectioned and stained with H and E for measures of infarct volume.

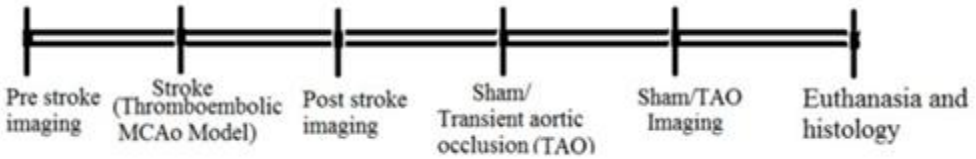

Figure 5. Timeline for LSCI study to observe hemodynamic changes during transient aortic occlusion (TAO) in thromboembolic model of stroke. The LSCI maps acquired at various time points shown on this timeline image were assessed to obtain the changes in anastomoses and blood flow diameter.

3.1.1. Dynamics of cerebral anastomoses during TAO in MCAo rats

An analysis of the number of anastomotic connections revealed that there was no variation in the number of anastomoses between MCAo + sham TAO and MCAo + TAO groups at post-stroke and post-treatment time points ($P>0.05$; n=5 per group, Figure 6)

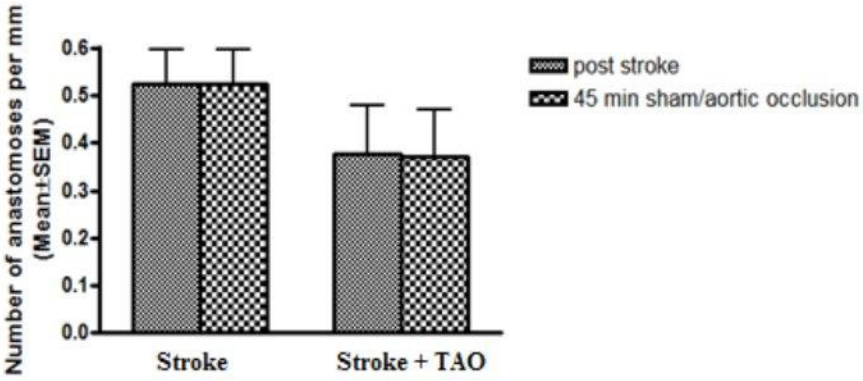

Figure 6. Change in number of anastomoses during treatment. The number of anastomoses adjusted to the length of the window did not change during post stroke and during sham/TAO treatment in MCAo and MCAo+ TAO groups (P>.05; n=5 per group). Data illustrated as mean ± s.e.m.

3.1.2. Characterisation of blood flow changes during TAO in MCAo rats

To more directly illustrate blood flow velocity changes due to TAO, $\tau_{baseline}$ / τ_c ratios (Figure 7A-B) were calculated within animals. Because τ_c are inversely proportional to blood flow velocity, these ratios illustrate blood flow velocity relative to baseline in post-MCAo (or sham-MCAo) and post-TAO (or sham-TAO) imaging sessions. Two-way RM-ANOVA confirmed a significant main effect of both treatment group ($F_{(3, 17)}$ = 9.708, P = 0.0006) and time ($F_{(1, 17)}$ = 17.32, P = 0.0007) on $\tau_{baseline}$ / τ_c ratios calculated post-MCAo (or sham) and post-TAO (or sham) in MCA segments, and a significant interaction between treatment group and time ($F_{(3, 17)}$ = 3.484, P = 0.0389).[96] Sidak's multiple comparisons revealed significant increases in blood flow during the 45th minute of TAO in these MCA branches in both MCAo and sham-MCAo groups (Figure 7A). Significant main effects of treatment group and time were also observed for surface veins (Figure 7B, *Treatment group*, $F_{(3, 17)}$ = 7.280, P = 0.0024; *Time*, $F_{(1, 17)}$ = 5.543, P = 0.0308), though Sidak's post hoc comparisons within groups did not reach significance. [96]

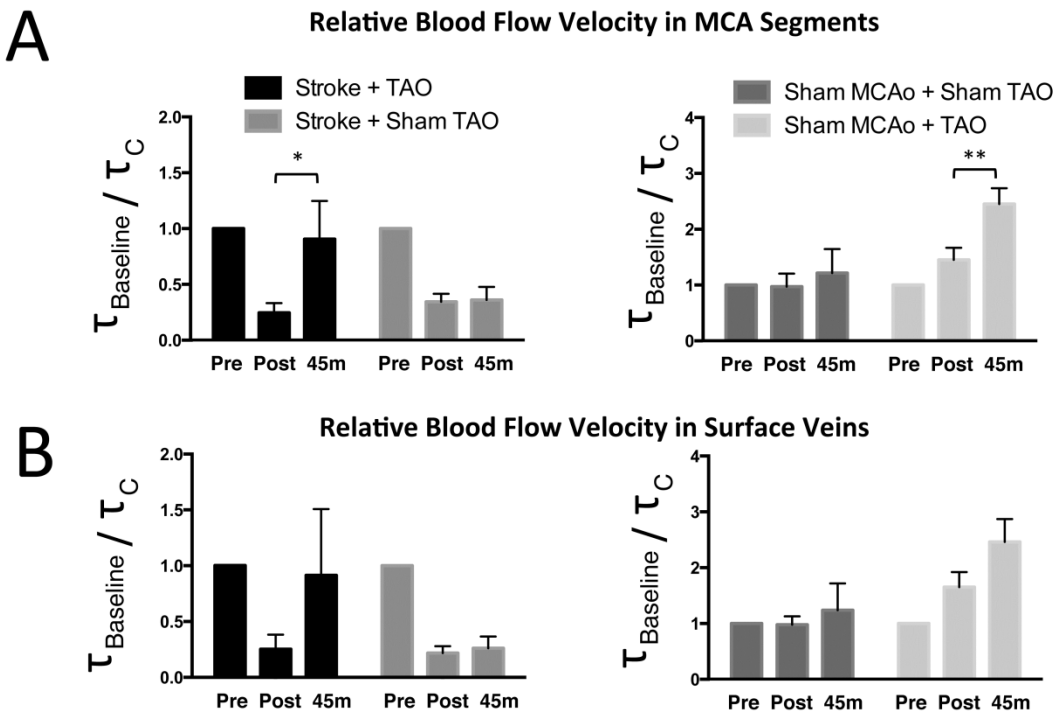

Figure 7. Elevated blood flow velocity during transient aortic occlusion (TAO) treatment of middle cerebral artery occlusion (MCAo). (A) Calculating the tbaseline/tc ratio within animals illustrates the velocity of blood flow in MCA segments downstream of leptomeningeal anastomoses during stroke and treatment relative to baseline measures (see Materials and Methods). Two-way repeated measure analysis of variance confirmed a significant main effect of both treatment groups ($F(3, 17)=9.708$, $P=0.0006$) and time ($F(1, 17)=17.32$, $P=0.0007$) on tbaseline/tc ratios in MCA segments, and a significant interaction ($F(3,17)=3.484$, $P=0.0389$). Notably, LSCI indicates that TAO induced a significant increase in blood flow velocity in MCA branches in both MCAo and sham-MCAo groups (Sidak's multiple comparison test, MCAo+TAO, *$P<0.05$; Sham-MCAo+TAO, **$P<0.01$). (B) A significant main effect of treatment and time was also observed for surface veins (Figure 4C, treatment group, $F(3, 17)=7.280$, $P=0.0024$; time, $F(1, 17)=5.543$,$P=0.0308$). A trend for enhanced blood flow velocity in surface veins in TAO-treated rats was apparent, though post hoc comparisons did not reach significance. Data illustrated as mean±s.e.m.[96]

3.1.3. Diameter changes of blood vessels during TAO in MCAo rats

The dilation of blood vessels was measured using Image J in LSCI maps obtained at pre-stroke, post-stroke and during TAO for all four groups as mentioned above. The diameter changes of blood vessels are given in Figure 8.

Two-way RM-ANOVAs of vessel diameter in surface vasculature revealed significant main effect of time in MCAo segments ($F_{(2, 32)} = 31.91$, $P < 0.0001$) and surface veins ($F_{(2, 30)} = 15.53$, $P < 0.0001$), and a significant interactions between treatment group and time (*MCA segments*, $F_{(6, 32)} = 10.91$, $P < 0.0001$; *surface veins*, $F_{(6, 30)} = 4.952$, $P = 0.0013$). Within group post hoc comparisons demonstrated that vessel diameters significantly increased in MCA segments downstream of ACA-MCA anastomoses after MCAo (Tukey's HSD, $P < .0001$) but not sham-MCAo ($P > .05$) (Figure 8A). Mean MCA segment diameter remained significantly greater than baseline and post-MCAo values during the 45th minute of TAO ($P < .0001$ and $P < .05$ respectively). Conversely, MCA diameters during the 45th minute of sham-TAO with MCAo were significantly smaller than post-MCAo values ($P < .0001$) and were not significantly different from baseline ($P > .05$). [96]

In surface veins, vessel diameters were significantly greater than baseline in both treated and untreated rats immediately after MCAo and during the 45th minute of TAO or sham-TAO ($P < .001$ for all comparisons; Figure 8B). Sham-MCAo rats did not show any significant changes in vessel diameter in either the TAO or sham-TAO groups (all $P > .05$).[96]

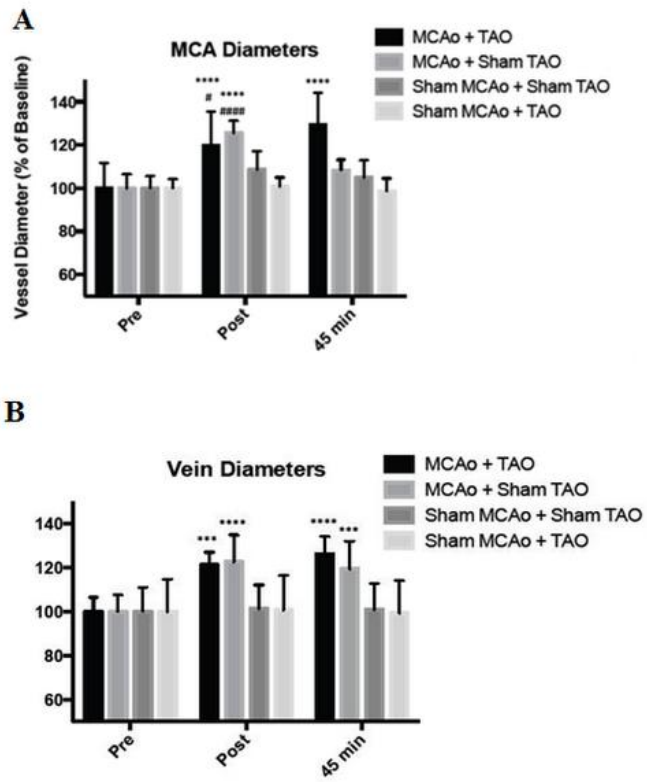

Figure 8. Effect of transient aortic occlusion (TAO) on vessel diameter during middle cerebral artery occlusion (MCAo). (A) Two-way repeated measure analysis of variances of vessel diameter in surface vasculature revealed significant main effect of time in MCAo segments ($F(2,32)=31.91$, $P<0.0001$) and surface veins ($F(2, 30)=15.53$, $P<0.0001$), and significant interactions between treatment group and time (MCA segments, $F(6,32)=10.91$, $P<0.0001$; surface veins, $F(6, 30)=4.952$, $P=0.0013$). Vessel diameters significantly increased in MCA segments downstream of ACA–MCA anastomoses in MCAo groups (Tukey's honestly significant difference, $P<0.0001$) but not sham-MCAo rats ($P>0.05$). However, MCA segment diameters remained significantly greater than baseline and post MCAo values during the 45th minute of TAO ($P<0.0001$ and $P<0.05$, respectively) whereas diameters during the 45th minute of sham-TAO with MCAo were significantly smaller than post MCAo values (Po0.0001) and were not significantly different from baseline (P40.05). (B) In surface veins, vessel diameters were significantly greater than baseline in both treated and untreated rats immediately after MCAo and during the 45th minute of TAO or sham-TAO ($P<0.001$ for all comparisons). * show significant differences between pre MCAo (baseline) measures and post MCAo values, whereas # shows differences between post MCAo values and measures in the 45th minute of TAO or sham-TAO (*$P<0.05$, **$P<0.01$,***$P<0.001$, ****$P<0.0001$).[96] Data illustrated as mean ± s.e.m.

3.1.4. Blood flow rate changes during TAO in MCAo rats

To better estimate the change in blood flow through the blood vessel due to TAO, incorporating both blood flow velocity and diameter changes, we calculated the relative blood flow rate (*relQ*).

Analysis of *rel Q* across treatment groups (Figure 9) revealed a significant main effect of treatment group ($F_{(3, 16)} = 3.506$, P = 0.0399") and time ($F_{(1, 16)} = 9.926$, $P = 0.0062$), and post hoc comparisons confirmed a significant increase in blood flow (*rel Q*) during TAO in the MCAo + TAO group (Sidak's multiple comparisons test, $P < .05$; all other comparisons $P > .05$). Notably, in the MCAo + TAO group, blood flow (*rel Q*) during TAO was 6.34 ± 2.37 fold greater than post-MCAo blood flow (Figure 9A), whereas blood flow (*rel Q*) MCAo + Sham-TAO was reduced during sham-TAO relative to post-MCAo (0.81 ± 0.21 fold change). A similar effect was observed in venous *Q* (Figure 9B), where *Q* values during TAO were 8.89 ± 4.25 fold greater than post-MCAo *Q*.[96]

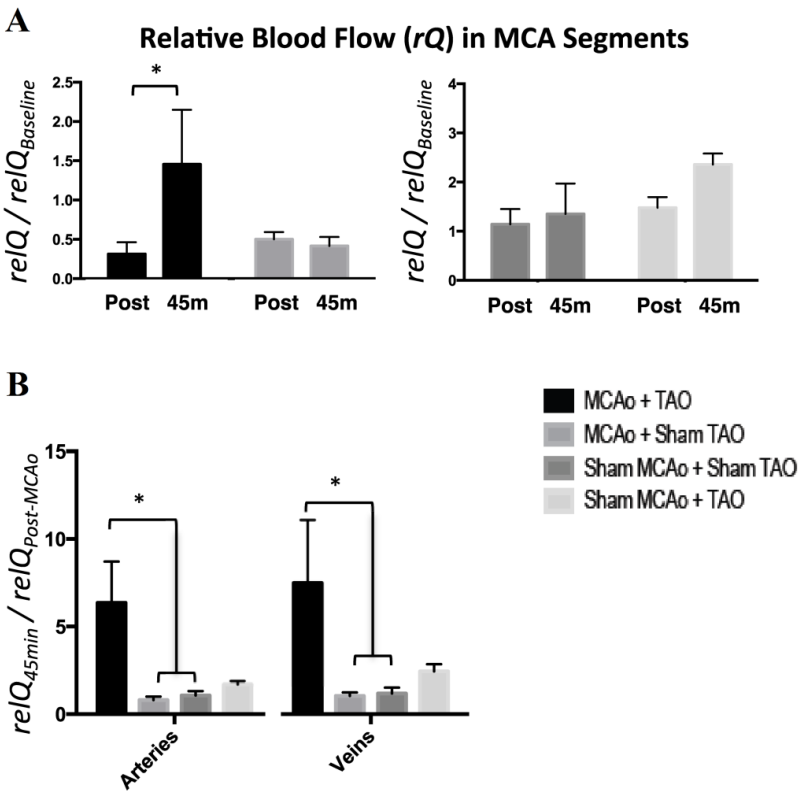

Figure 9. Effect of transient aortic occlusion (TAO) on blood flow during middle cerebral artery occlusion (MCAo). (A) To estimate blood flow through MCA segments due to TAO, incorporating both blood flow velocity and diameter changes, a measure of relative blood flow (relQ) during TAO (or sham) relative to postMCAo (or sham) was calculated (see Materials and Methods). Analysis of relQ across treatment groups revealed a significant main effect of treatment group ($F(3, 16)=3.506$, $P=0.0399$) and time ($F(1, 16)=9.926$, $P=0.0062$), and post hoc comparisons confirmed a significant increase in blood flow (relQ) during TAO in the MCAo+TAO group (Sidak's multiple comparison test, *$P<0.05$; all other comparisons $P>0.05$). (B) Determining the ratio of blood flow (relQ) during the 45th minute of TAO (or sham) relative to postMCAo (or sham) values gives an index of blood flow change due to treatment. This relQ ratio was significantly affected by treatment in both MCA segments (analysis of variance, $F(3, 16)=4.694$, $P=0.0155$) and surface veins ($F(3, 15)=3.938$, $P=0.0295$). Notably, in both MCA segments and surface veins, this relQ ratio was significantly greater in the MCAo+TAO group relative to MCAo+Sham-TAO and Sham-MCAo+Sham-TAO (Tukey's HSD, *Po0.05).[96] Data illustrated as mean±s.e.m.

3.1.5. Histology

LSCI maps of collateral blood flow provided conclusive evidence of MCAo. Nonetheless, to confirm ischemic damage due to thromboembolic MCAo consistent with our previous studies, [46] histological assessment of early infarct was performed on a subset of rats from imaging experiments (n = 6). H&E staining (Figure 10) demonstrated early indications of infarct in both TAO-treated and untreated MCAo rats (n = 3 from each TAO and sham treatment groups). Infarcts included regions of the striatum and/or overlying sensorimotor cortex ipsilateral to the occlusion, with a mean volume of 81.27 ± 41.57 mm^3. While neuroprotective efficacy was not a focus of this study, smaller early infarct in rats treated with TAO vs. sham (61.63 ± 46.68 mm^3 vs. 100.91 ± 31.37 mm^3, respectively) in this small subset of animals warrant further investigation to determine if infarct reduction is statistically significant when repeated in a larger cohort of animals.[96]

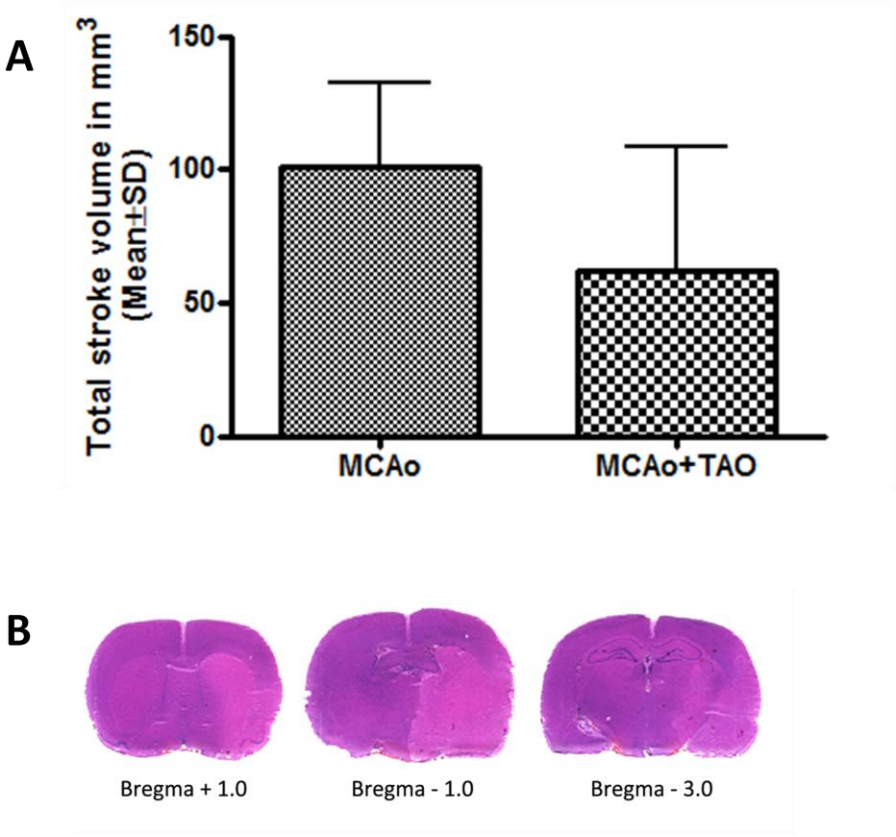

Figure 10. Early infarction volume measurements. (A) Early infarction volume in TAO and untreated rats expressed as mm^3. TAO slightly reduces infarction volume Vs Sham. However, statistical significance was not observed due to low statistical power (t-tests, $P>0.05$; $n=3$ per group). Data illustrated as mean ± s.d. (B) Representative image of H and E staining.

3.2. Long term neuroprotection offered by TAO

Nineteen Sprague Dawley rats used in the experiment were divided into MCAo + TAO (n=9), MCAo + no treatment groups (n=10). Briefly, the rats were anesthetized with 1.5% isoflurane and were subjected to MCAo followed by no treatment or TAO. Thromboembolic MCAo was performed as described earlier but with a smaller clot size to allow long term recovery (0.8cm).The brains collected from these rats after one week recovery was flash frozen and stored at -20 ^{o}C. The brains were sectioned and stained using cresyl violet staining.

The timeline for this experiment is given in Figure 11.

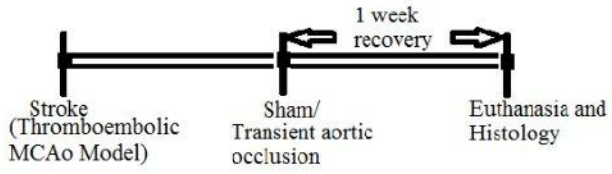

Figure 11. Timeline for assessing long term neuroprotection of TAO. The brains obtained from this experiment were flash frozen and sectioned to assess the final lesion volume using cresyl violet staining.

3.2.1. Histology

TAO treatment (relative to sham) did not offer statistically significant neuroprotection in our analysis of infarct volume at 1 week after stroke and treatment ($P > 0.05$; Figure 12). However, the variability of stroke size was a significant issue, as the small clot size required for long-term recovery

resulted in significant variation in final infarct volume. Interestingly, striatal infarct was not observed in any TAO treated rats (n=9), indicating that it may offer protection by shifting the clot past the lenticulostriatal arteries (Figure 13). A Fisher's Exact test on the presence or absence of striatal infarct suggests a significant difference between treatment groups ($P = 0.0031$). To focus on mechanisms unrelated to clot shift, our next studies used a filament model of MCAo.

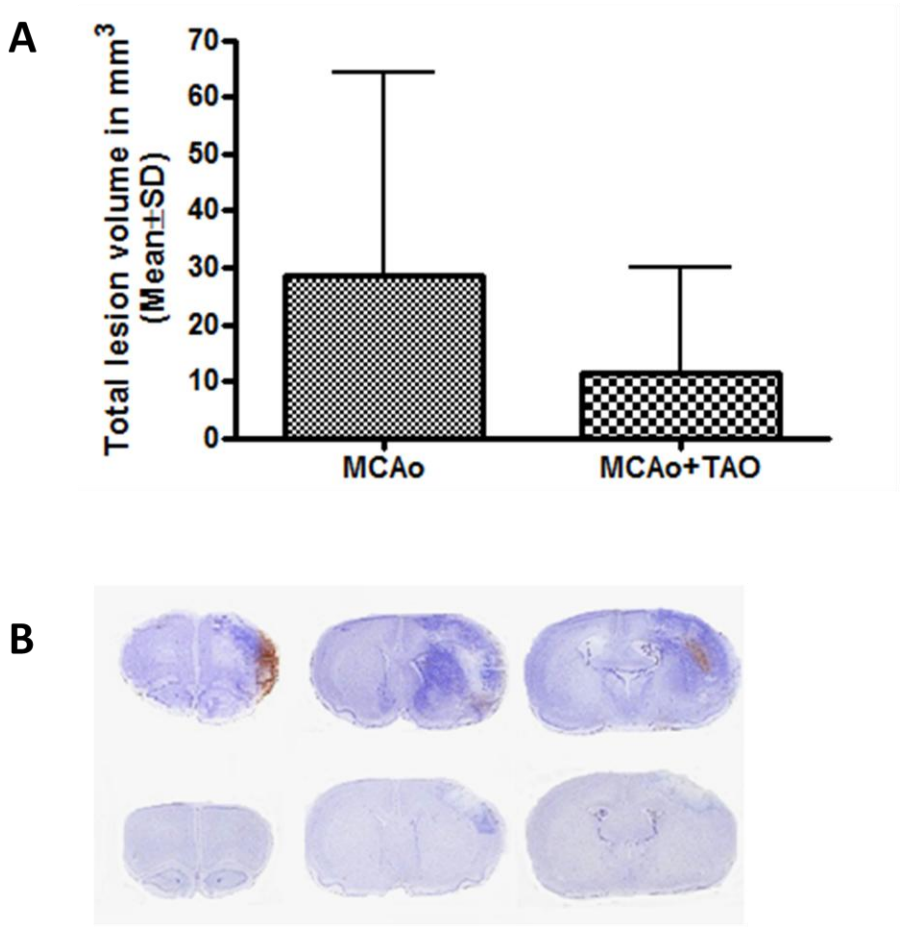

Figure 12. Total infarction volume measurements. (A)TAO seems to reduce infarction volume after thromboembolic MCAo; However it did not reach significance due to variability in infarct size (t-tests, $P > 0.05$; n=10 in MCAo group; n=9 in MCAo + TAO group). Data illustrated as mean ± s.d. (B) Representative image of cresyl violet staining showing large and small infarcts in this study.

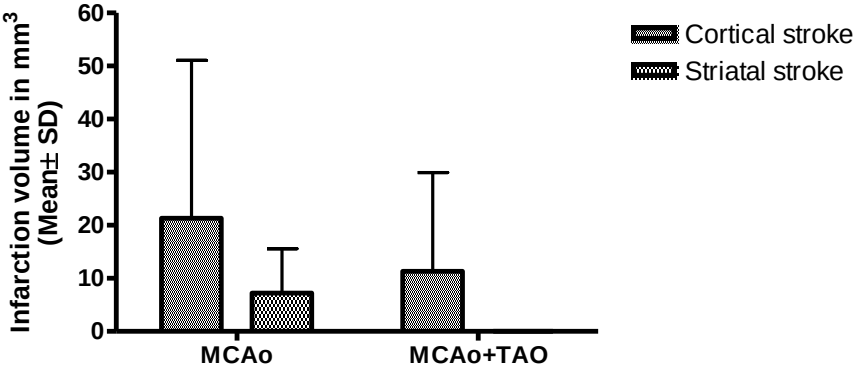

Figure 13. Cortical and striatal infarction volume measurements. The MCAo group has both cortical and striatal strokes. The MCAo +TAO group has cortical strokes alone (Two way ANOVA, P>0.05; n=9 per group). Data illustrated as mean ± s.d.

3.3. Persistent cortical blood flow changes after transient aortic occlusion during thromboembolic model of MCAo

In this aim, LSCI maps were acquired from the imaging experiment outlined in Figure 14 to confirm the persistence of cortical blood flow after TAO. Thromboembolic MCAo was used to induce stroke and was performed as described earlier but with a longer clotting time to prevent clot shifting (20 minutes clotting time). Five male Sprague Dawley rats (size: 400-550g) were used in this study.

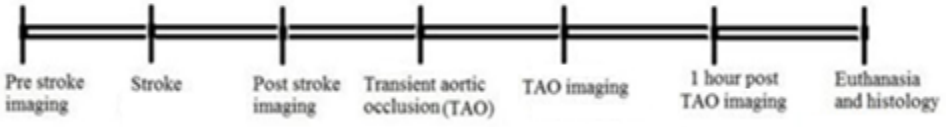

Figure 14. Timeline for LSCI study to observe hemodynamic changes after the TAO in thromboembolic model of stroke. The LSCI maps acquired at various time points shown on this timeline image were assessed to obtain the changes in blood flow velocity, blood vessel diameter and blood flow rate.

3.3.1. Blood flow rate changes during TAO in MCAo rats

In five animals, TAO induced changes were imaged 75 minutes after removal of the aortic catheter and balloon. LSCI maps demonstrated that enhanced collateral blood flow persisted through all imaging sessions in four of five rats (Figure 15A, large arrow), with two rats exhibiting a restoration of blood flow in MCA segments that were not carrying blood

after MCAo that persisted after catheter removal (e.g. Figure 15B, small arrows). MCAo + TAO induced persistent increases in blood flow, as *relQ* values calculated from MCA segments identified in images acquired 75 minutes after catheter and balloon removal were 3.30 ± 1.33 fold greater than post-MCAo values. Notably, this likely underestimates persistent TAO-induced changes in flow, as vessels that reperfused only after treatment were not included in these calculations because reliable measures of vessel diameter were not possible. [96]

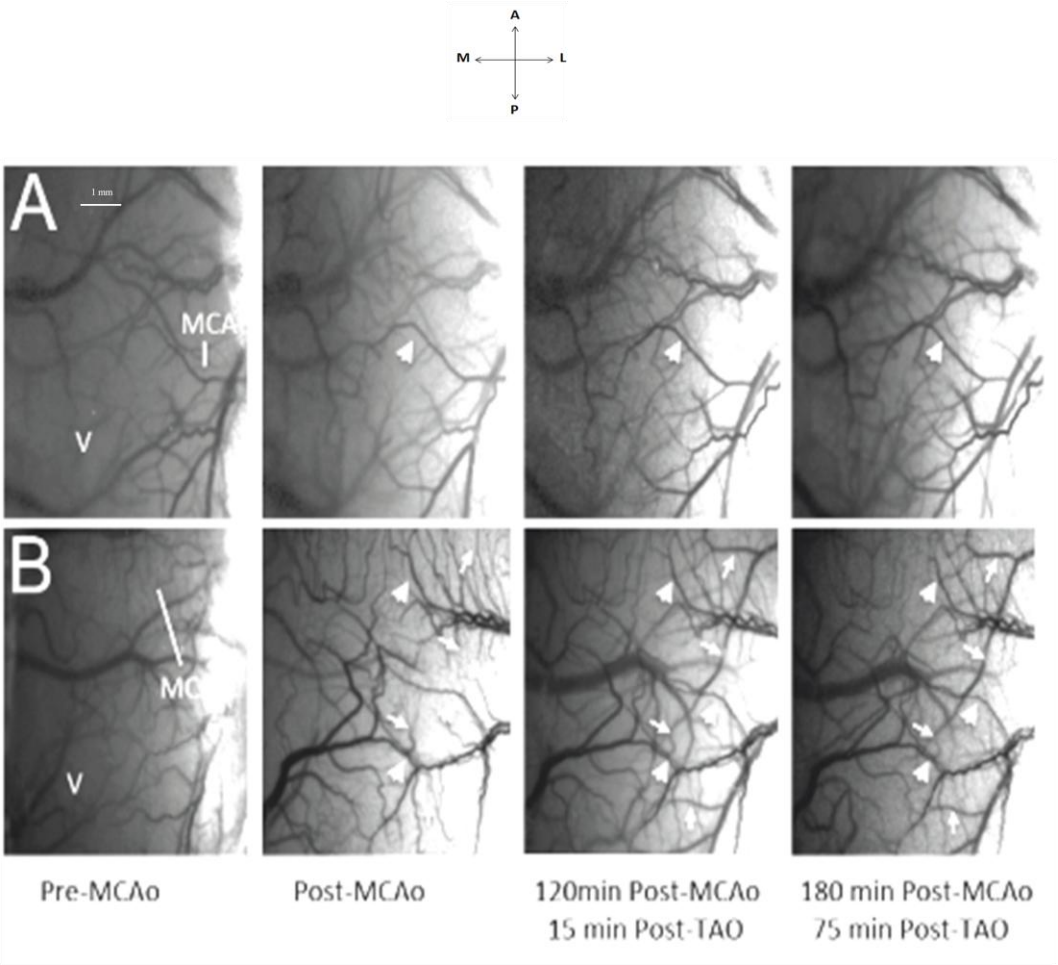

Figure 15. Persistent changes in blood flow after transient aortic occlusion (TAO). (A) Laser speckle contrast imaging after removal of the catheter suggests that TAO-induced increases in collateral blood flow persist after treatment (note darker middle cerebral artery (MCA) segments (arrowheads) downstream of anastomoses in panels indicating post TAO imaging relative to post MCAo (middle cerebral artery occlusion) imaging). (B) Notably, MCA segments not carrying blood after MCAo reperfused after TAO (see small arrows in second and third panel from left, persistent connections indicated by large arrowheads), perfusion in these vessels persisted 75 minutes after catheter removal (post TAO images at right).A, Anterior; P, Posterior; M, Medial; L, Lateral. [96]

3.4 Persistent cortical blood flow dynamics after transient aortic occlusion in a filament model of MCAo

In this aim, LSCI data acquired from the imaging experiment timeline illustrated in Figure 16 was analyzed to better describe the change in blood flow after TAO during filament model of MCAo. Twenty six male Sprague Dawley rats (Size 400-450g) were used in this study. They were divided into two treatment groups (MCAo + TAO, MCAo + Sham TAO) prior to LSCI through a thin-skull imaging window.

LSCI maps acquired from this experiment were analyzed to determine the correlation times for the blood vessels at different time points, the diameter of the blood vessels in the imaging window and blood flow rate across the blood vessels. The brains obtained from this experiment were sectioned and stained with H and E for measures of infarct volume.

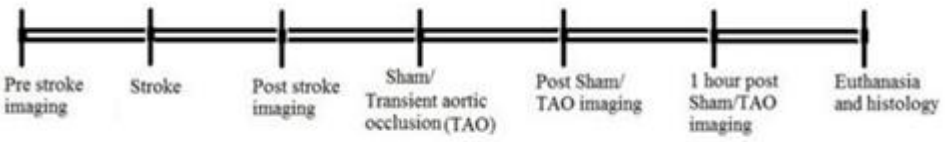

Figure 16. Timeline for LSCI study to observe hemodynamic changes after the TAO in filament model of stroke. The LSCI maps acquired at various time points shown on this timeline image were assessed to obtain the changes in blood flow velocity, blood vessel diameter and blood flow rate.

3.4.1. Mortality rate and physiological parameters after sham/ transient aortic occlusion in filament model of MCAo

The physiological parameters recorded using pulse oxymetry during the experiment are given in Table 1. Mortality rate in these rats was higher than the thromboembolic study due to the greater ischemia induced by the proximal occlusion (likely blocking flow through ACA and MCA, Table 2). Notably, a trend towards higher mortality rate after proximal MCAo in sham treated rats as compared to TAO-treated rats was apparent (Fisher's Exact Test, $P = 0.090$).

Parameter	Group	Pre-stroke	Post-stroke	Post-treatment	1hr post-treatment
Arterial O_2 Saturation	TAO	98.82957 ± 0.3837	98.83591 ± 0.1381	95.97681 ± 0.9296	95.22703 ± 1.417
	Sham	99.08818 ± 0.3401	99.18249 ± 0.2156	98.20252 ± 1.077	92.8821± 5.0192
Heart rate	TAO	366.753± 10.6917	389.537± 11.9145	404.4024 ± 13.1468	414.2968 ± 20.9385
	Sham	386.7578 ± 20.6593	414.1389 ± 20.2803	381.0123 ± 31.1779	439.3498 ± 22.2905
Breath rate	TAO	100.4284 ± 5.9192	96.5302± 6.5562	96.98679 ± 5.6786	82.52425 ± 3.5397
	Sham	97.54727 ± 6.7961	89.57752 ± 3.2198	94.99104 ± 8.8511	85.52333 ± 2.4592

Table 1. Physiological parameters measured at different time points in both the treatment groups. Data illustrated as mean ± s.e.m. Two-way RM-ANOVA showed a significant main effect of time in arterial O_2 saturation, heart rate, breath rate ($F_{(3, 30)} = 5.45$, $P = 0.0041$; $F_{(3, 30)} = 4.08$, $P = 0.0152$; $F_{(3, 30)} = 4.47$, $P = 0.0104$) respectively and insignificant effect of treatment.

Groups	Mortality/ (Total number of animals)
Prior to treatment	**5** /26
Sham treatment	4/11
TAO	0/10

Table 2. Rates of mortality in different groups during and prior treatment. Mortality rate after proximal MCAo appears higher in sham treated rats (Fisher's Exact Test, $P = 0.090$).

3.4.2. Changes in relative blood flow velocity after transient aortic occlusion in filament model of MCAo

The LSCI maps after treatment or sham treatment appear darker, suggesting that blood flow improves over time during both sham treatment and TAO (Figure 17). Interestingly, this was in accordance with the analysis the speckle contrast factor (K) across various time points for measuring the blood flow. This speckle contrast value was converted to correlation times (τ_c) which are inversely and linearly proportional to blood flow velocity.[107] To more directly illustrate blood flow velocity changes in MCA segment due to TAO, $\tau_{baseline} / \tau_c$ ratios (Figure 18A) were calculated within animals. Because τ_c are inversely proportional to blood flow velocity, these ratios illustrate blood flow velocity relative to baseline in post-MCAo, post-TAO(or sham-TAO) and 1hour post-TAO(or 1 hour sham-TAO) imaging sessions.

Two-way RM-ANOVA did not show a significant main effect of treatment in the MCA segment ($F_{(1, 30)} = 0.34$, $P > 0.05$). The blood flow velocity of MCA segments decreased after filament MCAo and increased after both TAO and Sham treatment (n=10 in TAO group; n=7 in Sham TAO group). This persistent increase in blood flow velocity was maintained even one hour after the cessation of the TAO/Sham treatment. However, the blood flow drop after MCAo was different between MCAo + Sham and MCAo +

TAO groups. After a filament model of MCAo, the MCA blood flow dropped to 22.16 ± 7.60% of the baseline value in MCAo + TAO group and to 40.04 ± 8.29% of baseline flow in MCAo + Sham group. Lower blood flow prior to treatment in the TAO group may reflect higher mortality in the sham treated group (where animals with more severe ischemia did not survive to experiment completion). To evaluate changes in blood flow velocity due to treatment group, $\tau_{Post\text{-}stroke} / \tau_c$ was obtained as illustrated in Figure 18 B. When τ_c was normalized to post stroke values an increase of 6.22 ± 2.30 in MCA velocity was suggested in MCAo + TAO group when compared with 1.61 ± 0.35 increase in MCAo + Sham group.

Two-way RM-ANOVAs of $\tau_{Post\text{-}stroke} / \tau_c$ in surface vasculature did not reveal a significant main effect of treatment in MCAo segments ($F_{(1, 15)}$ = 2.44, $P > 0.05$) and an insignificant interactions between treatment group and time.

A similar trend was observed in measures of blood flow velocity in the surface veins (Figure 19). Two-way RM-ANOVAs of $\tau_{Post\text{-}stroke} / \tau_c$ in surface veins did not reveal a significant main effect of treatment ($F_{(1, 15)}$ = 1.84, $P > 0.05$), and a insignificant interactions between treatment group and time.

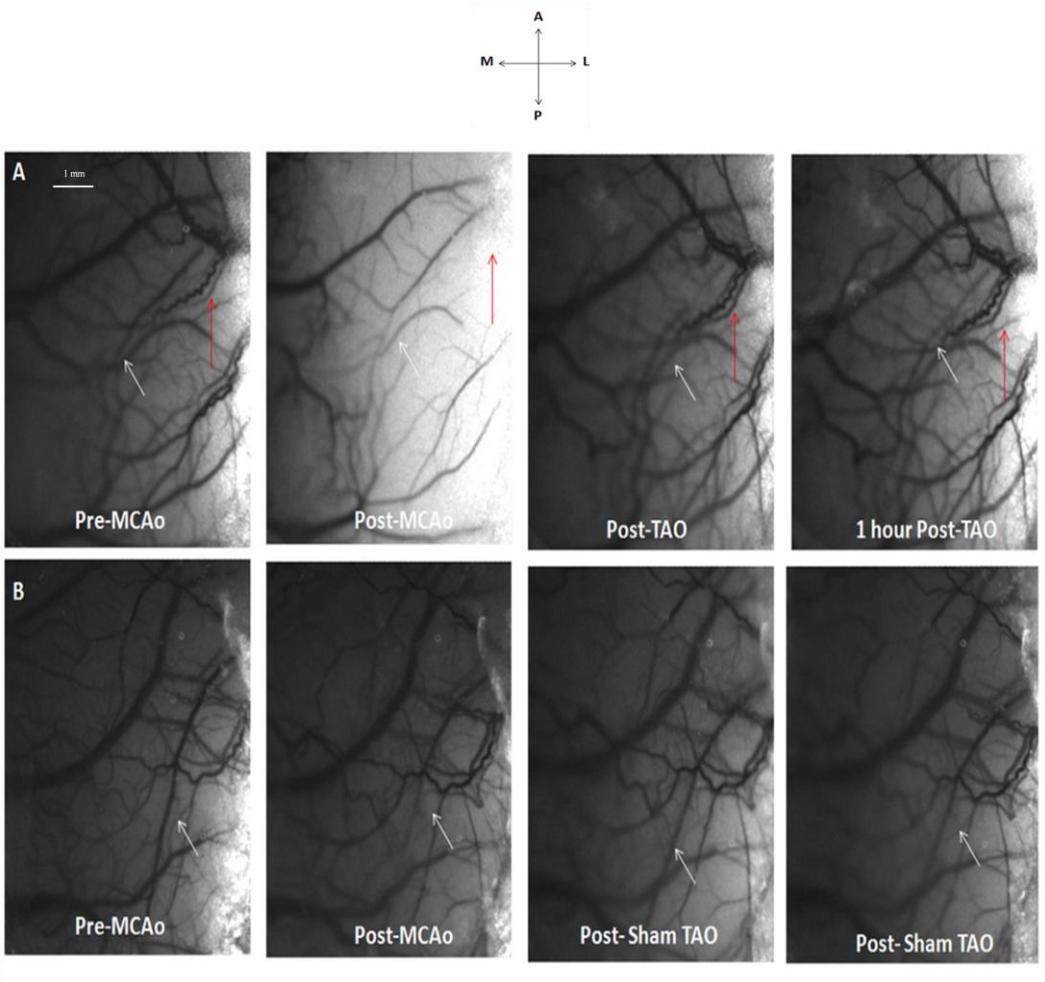

Figure 17. Mapping blood flow after focal ischemic stroke and after treatment using LSCI in filament model of MCAo. LSCI image showing blood flow in surface veins and distal branches of MCA over the hindlimb and forelimb sensory motor cortex. White arrows indicate the blood flow through the anastomotic connections between the distal branches of MCA and ACA after MCAo and persistence of anastomoses in post treatments. Red arrows indicate the blood vessels which disappeared after MCAo and reappeared after TAO treatment. (A) The first (from left) and second panels show blood flow changes before and after MCAo, whereas the third and fourth panel show blood flow changes immediately after TAO and one hour post TAO. (B) The first and second panels show blood flow changes before and after MCAo, whereas the third and fourth panel show blood flow changes immediately after sham TAO and one hour post sham TAO. A, Anterior; P, Posterior; M, Medial; L, Lateral.

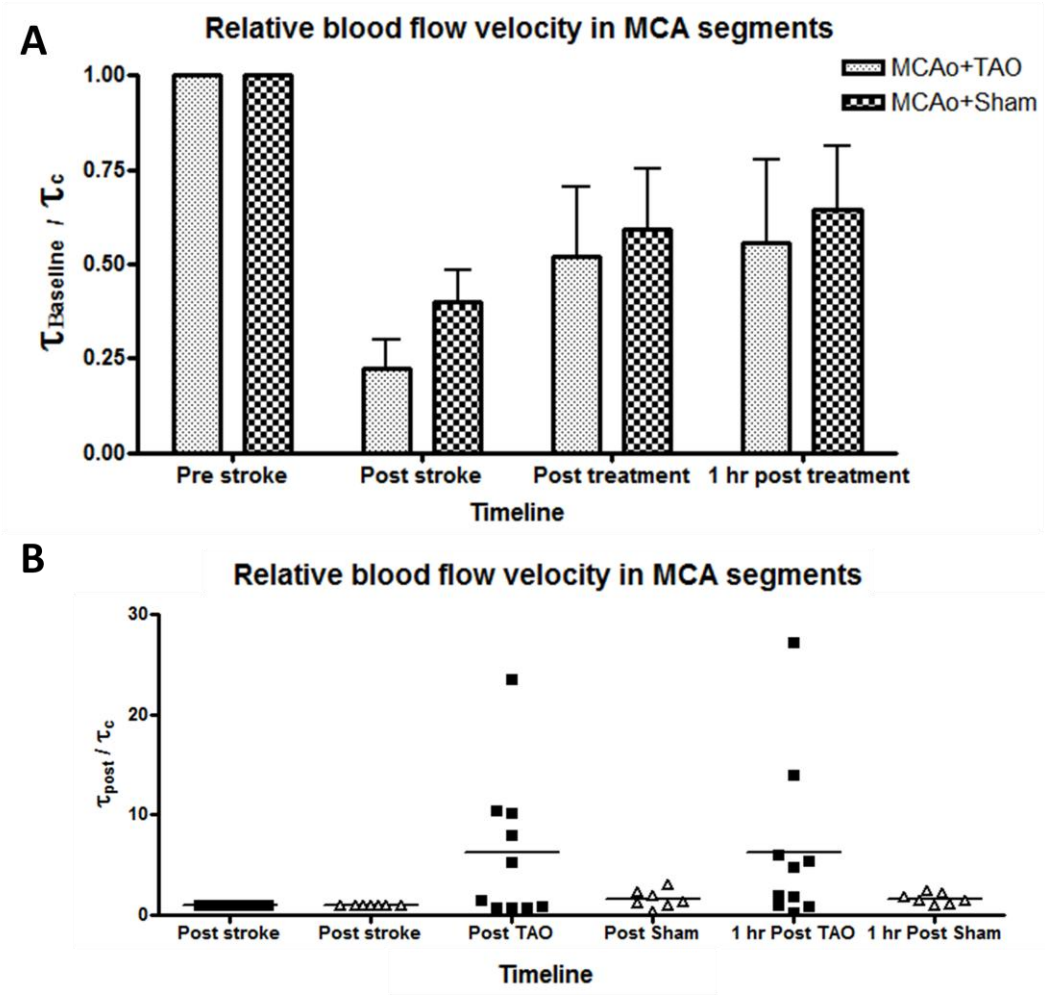

Figure 18. Mean changes in MCA blood flow after treatment. $\tau_{Baseline} / \tau_c$ depicts the velocity changes within the blood vessel relative to the baseline blood flow. (A) $\tau_{Baseline} / \tau_c$ in the MCA segment increased during both TAO and sham treatments (RM ANOVA, ($P > 0.05$). (B) $\tau_{Poststroke} / \tau_c$ in the MCA segment shows increased blood flow after TAO treatment while sham TAO group did not show any such change (RM ANOVA, $P > 0.05$; n=10 in Stroke + TAO, n=7 in Stroke + sham). Data illustrated as mean ± s.e.m.

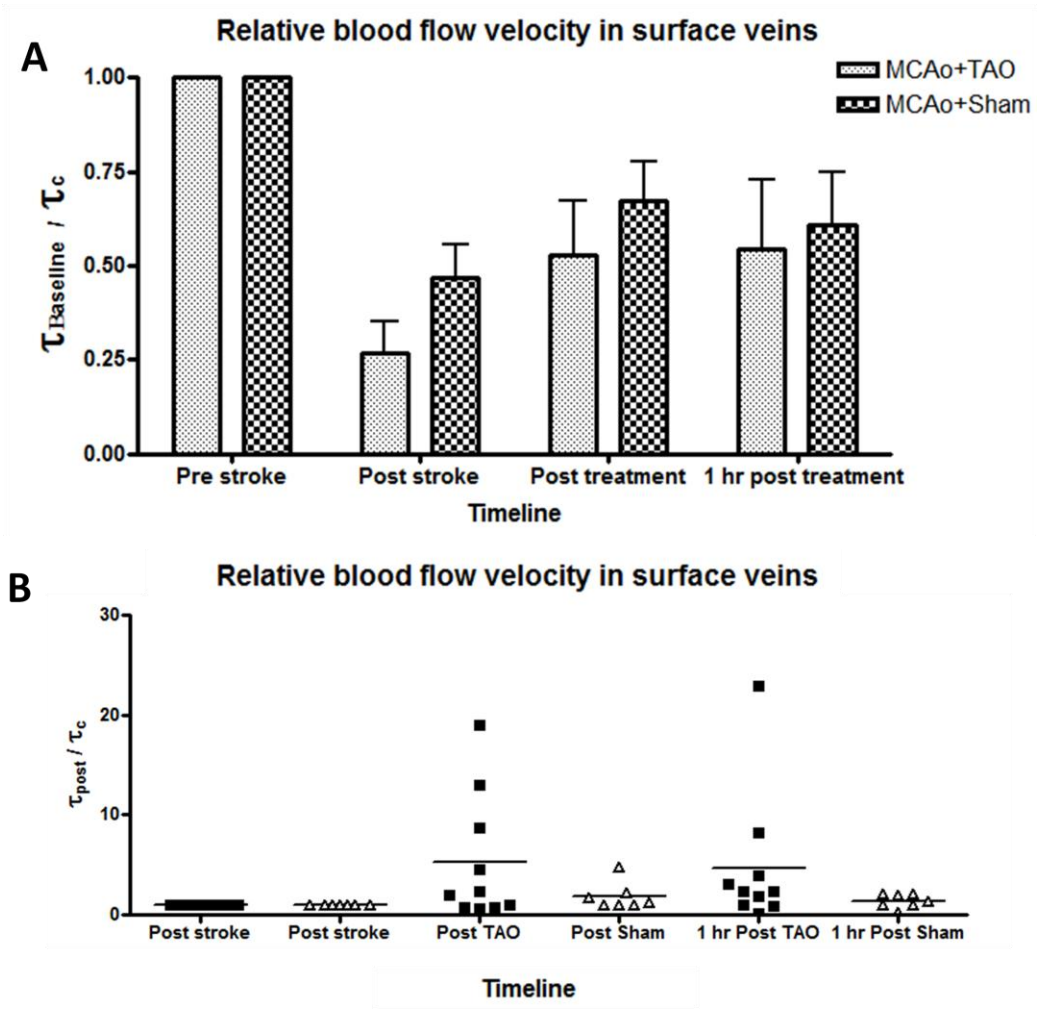

Figure 19. Mean changes in venous blood flow after treatment. $\tau_{Baseline} / \tau_c$ depicts the velocity changes within the blood vessel relative to the baseline blood flow. (A) The $\tau_{Baseline} / \tau_c$ of surface veins increased during both TAO and sham treatments (RM ANOVA, $P > 0.05$; n=9 in Stroke + TAO, n=7 in Stroke + sham). (B) $\tau_{Poststroke} / \tau_c$ of the surface veins increased during both TAO and sham treatments (RM ANOVA, $P > 0.05$; n=10 in Stroke + TAO, n=7 in Stroke + sham). Data illustrated as mean ± s.e.m.

3.4.3. Changes in relative blood flow diameter after transient aortic occlusion in filament model of MCAo

Since the borders of blood vessels were not apparent immediately after MCAo, due to the severity of the ischemia induced, diameter measures could not be reliably determined at the post-MCAo time point. An increase in blood flow over time was apparent in both treated and untreated rats was apparent over time, and vessel boundaries could be determined in most rats at later time points. Hence, the diameters of the blood vessels at baseline and after treatment were measured using the Image J plug-in. The dilation due to treatment is illustrated as a ratio of diameter of 1 hour post-treatment to diameter at baseline ($D_{1\text{ hour post treatment}} / D_{\text{baseline}}$). $D_{1\text{ hour post treatment}} / D_{\text{baseline}}$ for MCA segments and surface veins in MCAo + TAO group were 1.13 ± 0.05 and 1.07 ± 0.09 respectively. But, $D_{1\text{ hour post treatment}} / D_{\text{baseline}}$ for MCA segments and surface veins in MCAo + Sham group were1.02 ± 0.08 and 1.00 ± 0.07 respectively (Figure 20, $P > 0.05$; t-tests).

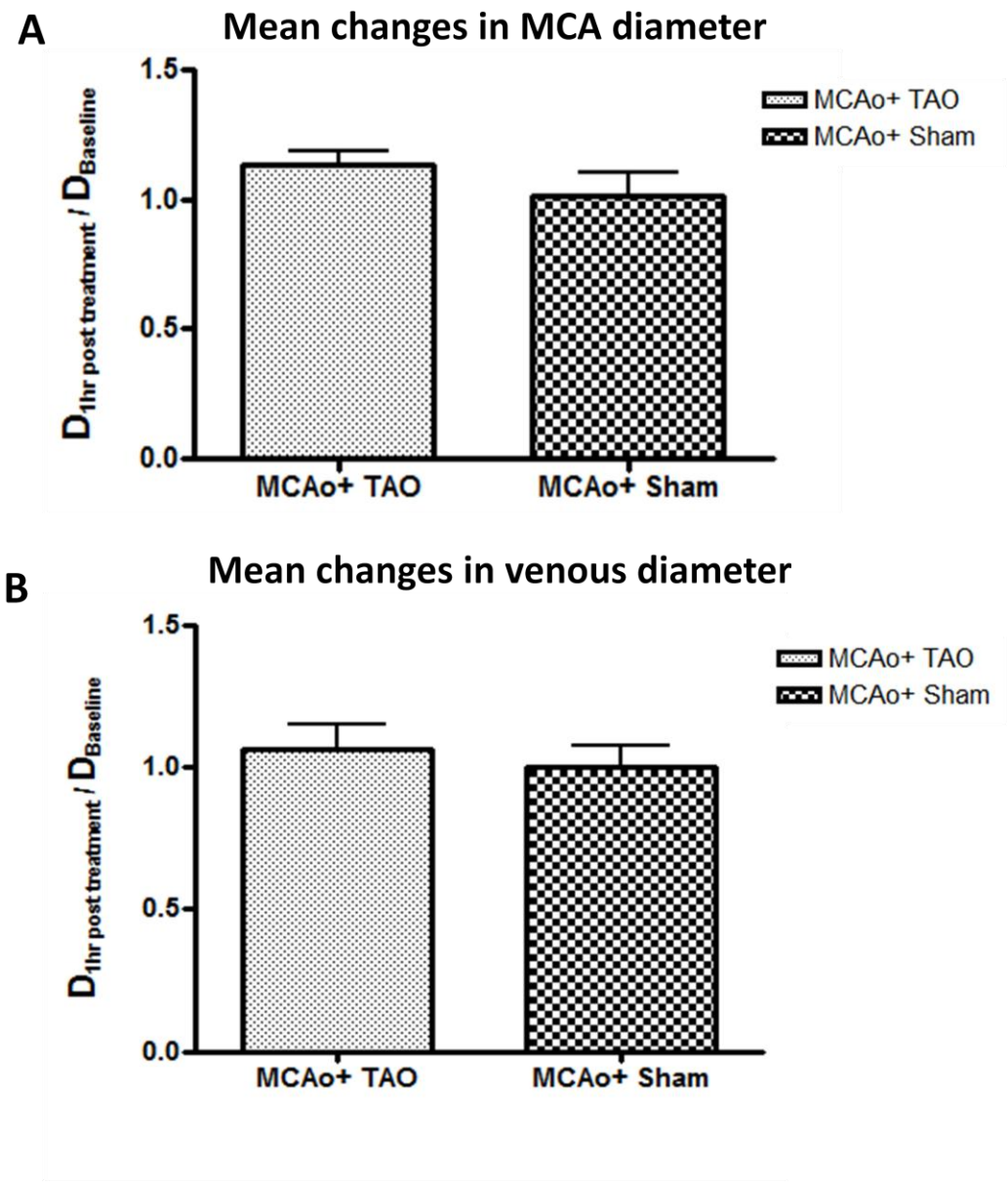

Figure 20. Mean changes in vessel diameter after treatment. $D_{1\text{ hour post treatment}} / D_{\text{baseline}}$ shows the changes in dilation after treatment. (A) $D_{1\text{ hour post treatment}} / D_{\text{baseline}}$ in the MCA segment shows a slight increase in dilation after TAO (t-tests, $P > 0.05$; n=10 in Stroke + TAO, n=7 in Stroke + sham). (B) $D_{1\text{ hour post treatment}} / D_{\text{baseline}}$ in the surface veins show a slight increase in dilation after TAO (t-tests, $P > 0.05$; n=10 in Stroke + TAO, n=7 in Stroke + sham). Data illustrated as mean ± s.e.m.

3.4.4. Changes in relative blood flow rate after transient aortic occlusion in filament model of MCAo

The blood flow rate measurements were obtained by using the formula

$$rel\ Q = \pi r^2(\tau_{Baseline} / \tau_c)$$

where *r* is the mean radius of the blood vessel in a given animal normalized to the baseline radius for that animal.

Analysis of *rel Q* reveals that the blood flow rate of the MCA segments and surface were not significantly different between treatment groups (Figure 21A and B, $P>0.05$; t-tests).

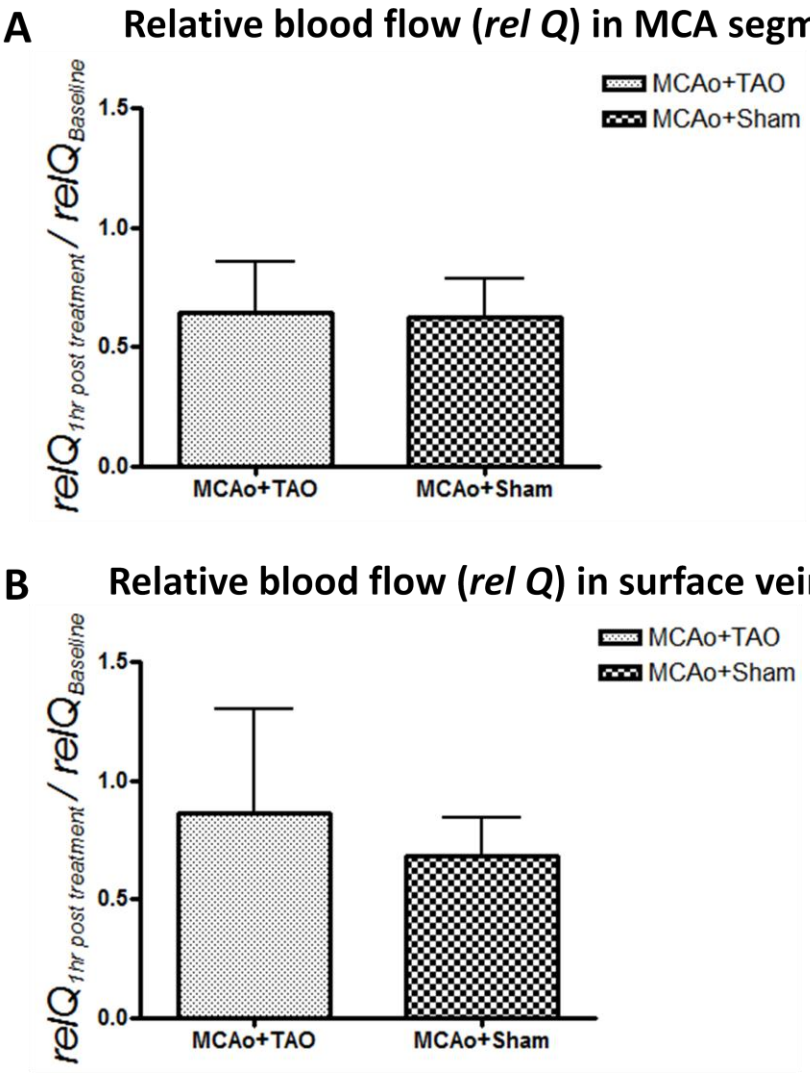

Figure 21. Mean changes in blood flow rate after treatment. It shows a measure of blood flow rate ratio (*rel Q*) at 1 hour after treatment relative to its baseline measure. (A) It shows $relQ_{1\ hour\ post\ treatment} / relQ_{prestroke}$ in the MCA segment in both TAO and sham TAO treatments. There was no significant difference in MCA blood flow rates after the treatments (t-tests, $P > 0.05$; n=10 in Stroke + TAO, n=7 in Stroke + sham). (B) It shows the $relQ_{1\ hour\ post\ treatment} / relQ_{prestroke}$ in the surface veins of both TAO and sham treatments. There was no significant difference in venous blood flow rates after the treatments (t-tests, $P > 0.05$; n=10 in Stroke + TAO, n=7 in Stroke + sham). Data illustrated as mean ± s.e.m.

3.4.5. Histology

The ischemic damage due to filament model of MCAo was confirmed by histological assessment of early infarct on a subset of rats from imaging experiments (*n* =10 in MCAo + TAO; n=7 in MCAo + Sham). H&E staining (Figure 22) demonstrated early indications of infarct in both TAO-treated and untreated MCAo rats. Infarcts included regions of the striatum and/or overlying sensorimotor cortex ipsilateral to the occlusion, with a mean volume of 87.46 ± 76.39 mm^3. Due to the variability in infarct size, no change in early infarction volume was observed in rats treated with TAO vs. sham (84.45 ± 68.72 mm^3 vs. 91.77 ± 91.87 mm^3, respectively). Given the differences in pre-treatment blood flow (with higher flow in the sham group), the lack of significant difference is not surprising.

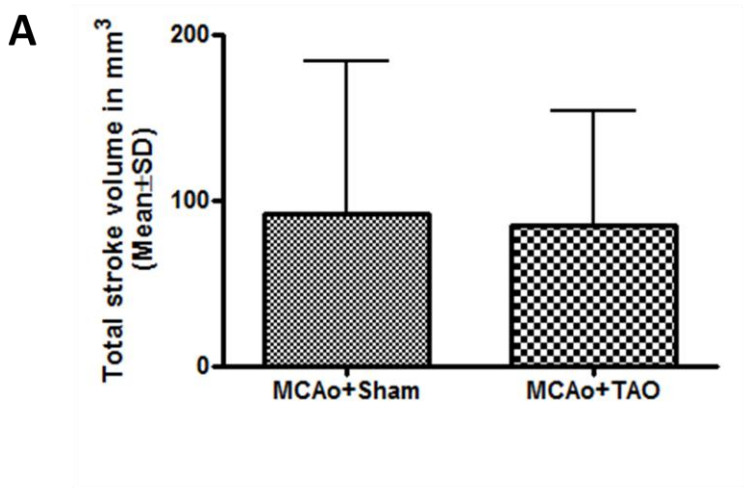

Figure 22. Early infarction volume measurements. (A)TAO shows a trend in reducing early infarction volume (t-tests, $P > 0.05$; n=9 in Stroke + TAO, n=6 in Stroke + sham). Data illustrated as mean ± s.d. (B) Representative image of H and E staining.

CHAPTER 4

Discussion

4.1. Overview

Our data shows persistent increases in blood flow downstream of ACA-MCA anastomoses after thromboembolic MCAo treated with TAO. The data shows that TAO restored blood flow in MCA segments downstream of leptomeningeal anastomoses to baseline levels and maintained stroke-induced vasodilation in these MCA segments (whereas vessel diameters in sham-treated rats returned to baseline within 45 minutes) and also suggests that the treatment may be neuroprotective early after ischemia.[96] Findings also suggest that TAO reduces the occurrence of striatal infarction after MCAo, possibly by moving the clot past the lenticulostriate arteries. Our data also show that the blood flow increases persist even after the removal of the aortic catheter. During proximal MCAo induced by a filament model, TAO appeared to reduce the stroke related mortality and demonstrated variable increases in collateral blood flow of cortical surface vessels.

4.2. TAO augments collateral blood flow during thromboembolic MCAo

rt-PA improves the cerebral perfusion by thrombolysis and is the only approved treatment for ischemic stroke.[17] However, due to its short therapeutic window and risk of hemorrhagic transformation less than 5% of the population in United States, and even fewer in other parts of the world, are treated with rt-PA.[23] The limitations of tPA as a treatment for ischemic

stroke necessitates the development of new approaches including augmenting cerebral collateral circulation during stroke. As mentioned previously, collateral circulation partially restores blood flow to the ischemic penumbra during an ischemic stroke. Augmenting blood flow through this collateral circulation might increase blood flow to ischemic territories during stroke, thereby reducing stroke deficits.[37] One such approach to augment collateral circulation is through TAO, in which the descending aorta is partially occluded using an inserted catheter to redistribute the systemic blood flow from the splanchnic circulation of lower torso to the upper torso and head.[111]

In this thesis we tested the ability of TAO to increase blood flow in a pair of rodent models of MCAo.

LSCI maps were analyzed to determine the changes in cortical blood flow dynamics and blood flow rate during TAO after thromboembolic MCAo in rats. LSCI provides high-resolution maps of blood flow on the cortical surface based on the blurring of speckle pattern due to the motion of blood cells. [106] While sensitive mapping of blood flow in surface vasculature is permitted by LSCI, the exact quantitative relationship between speckle contrast and blood flow velocity remains undefined. [97] The demonstration that correlation times are inversely proportional to blood flow is rooted in a

number of simplifying assumptions based on literature from other imaging modalities and may not hold under all imaging and blood flow conditions.[109]

Recent developments in LSCI image acquisition and analysis can improve quantitative accuracy, though at this point LSCI remains a powerful but only semi-quantitative modality best restricted to describing relative changes in blood flow within animals rather than a quantitative measure of blood flow velocity.[109, 112, 113] For this reason, our analysis focused on within animal data to demonstrate the relative blood flow changes with respect to baseline levels rather than demonstrating the quantitative measure of blood flow velocity.[96] Our data shows no difference in the number of anastomoses after TAO. However, in a thromboembolic stroke, the blood flow velocity as indicated by correlation times is significantly increased during TAO treatment.

Additionally, we noted that the arterial branches of MCA dilate after stroke in both treated and untreated rats. In the sham treated group this arterial dilation after stroke decreases to pre stroke level by the 45th minute. Contrary to this, the MCA branches were further dilated during TAO treatment and remained significantly greater than baseline and post-MCAo values during the 45th minute of TAO. In surface veins, vessel diameters

were significantly greater than baseline in both TAO and sham TAO rats immediately after MCAo and during the 45th minute of TAO or sham-TAO. No changes in dilation were observed in arteries and veins of animals after sham MCAo or Sham TAO. The mechanisms of dilation remain undefined, but may result from increased perfusion pressure or blood volume. Alternatively, this vasodilation due to TAO might be due to circulating vasoactive factors initiated by peripheral ischemia, as it has been observed after remote ischemic conditioning in patients with subarachnoid haemorrhage.[114]

The early infarction volume data suggests that TAO may reduce infarction volume early after ischemia in this model. However, due to low statistical power (n=3), the changes in infarction volume will need to be replicated in a larger sample of rats.

4.3. TAO might shift the clot in smaller sized strokes

A previous study of TAO in rodents showed a decreased infarction volume at 24 hours after stroke and synergistic reductions when combined with tPA.[93] In this study we assessed the effectiveness of TAO in reducing infarction volumes after thromboembolic model of ischemic stroke at one week after ischemic onset.

The final infarction volume data from thromboembolic model suggests a

slight reduction in infarction volume after TAO. However, the strokes induced by this thromboembolic MCAo are extremely variable and the changes in infarction volume did not reach significance. Interestingly, when this data was subdivided based on the location of infarction, we found that TAO offered complete protection to striatum and were associated only with cortical strokes. TAO might shift the clot past the lenticulostriatal arteries to protect the striatum with small clots, a novel neuroprotective mechanism that has not previously been demonstrated. However, this clot shift mechanism remains speculative, as the clot location was not confirmed directly by dissection of the blood vessel.

4.4. Persistence of cortical blood flow and neuroprotection after TAO in thromboembolic and filament model of MCAo

As described previously, TAO increased blood flow rate by dilating MCA in a thromboembolic MCAo in rats. However, the persistence of these blood flow changes was not known. Here, we examined the efficacy of TAO in inducing persistent changes in cerebral perfusion during occlusion of MCAo using the thromboembolic and filament models.

The results show that enhanced collateral blood flow persisted for at least 75 minutes after removal of the aortic catheter and balloon after thromboembolic MCAo.[96] These persistent increases in cerebral blood flow

agree with previous studies in a non-ischemic porcine model.[92]

In a filament model of MCAo, the increase in blood flow after TAO is apparent only when the blood flow is normalized to post-stroke measures. Blood flow in MCA segments downstream of anastomoses was lower immediately after MCAo in the TAO group when compared to the sham groups. This discrepancy likely results from the higher mortality in the sham treated group, since the rats with early mortality had more severe ischemia. We suggest that TAO increases blood flow sufficiently to permit survival through experiment completion even in severely ischemic rats. However, untreated rats do not survive, so only rats with more moderate ischemia were included in the sham treatment data. This postulation is supported by comparison of blood flow measures normalized to post-stroke values, which suggest a greater increase in blood flow over time in the treated group. Nonetheless, this presents confound for interpretation of these data. Future studies will need to focus on incorporation of a permanent distal occlusion model to prevent the difference in severity between the groups.

Due to the severity of stroke, diameter measurements could not be obtained immediately post-MCAo onset. In spite of the increased severity of stroke, the diameter of MCA and veins measured at 1 hour post treatment (or 3

hours post-MCAo) did not exhibit a clear dilation after treatment and the relative blood flow *(relQ*) measured at 1 hour post treatment (normalized to pre stroke level) did not show a significant change due to TAO treatment. However, the proximal MCAo model used in this study caused a difference in the pre-treatment severity of stroke between groups. Again, a distal model of MCAo to produce a permanent distal occlusion (cortical) would permit a less ambiguous assessment of blood flow changes due to treatment.

TAO reduced stroke induced mortality in this filament model of MCAo, in agreement with the clinical study by Shuaib et al [98] which showed that in patients with severe stroke, the TAO-treated patients were more likely to be free from stroke related mortality than the untreated patients. Clinical studies suggest that patients with moderate stroke benefit the most from TAO. The plausible explanation for this could be that patients with mild strokes tend to recover without treatment while those with severe stroke have extensive injury making their recovery less likely despite any treatment.[115] The results from our studies are in accordance with clinical data, as more moderate strokes (thromboembolic study) treated with TAO exhibited less ambiguous improvements in collateral blood flow than more severe (proximal) filament strokes. Moreover, filament MCAo can occlude both ACA and MCA; therefore, blood flow to MCA might come through

the Circle of Willis taking a more circuitous route. The results from these experiments reinforce the importance of patient selection in evaluation of new therapies for ischemic stroke and the impact of initial stroke severity on outcome.

4.5. Limitations

Several trials of neuroprotectants in acute stroke patients have resulted in unsuccessful or mixed outcomes and have reinforced the difficulties in translating the animal stroke studies into the clinic. [15, 16] In response to tackle the challenge, stroke treatment academic industry roundtable (STAIR) have questioned the relevant use of experimental animals (eg: age, sex, comparitive anatomy, comorbidities, sample sizes), stroke model (anesthesia, reperfusion, hypothermia), outcome measures (histology, functional outcome, morbidity), study quality (blinding, randomisation), dosing (appropriate dosing, time window) and patient selection.[116]

Consistent with the STAIR criteria, multiple models were used to evaluate the efficacy of TAO in rats.[117] However, the thromboembolic models results in variable infarcts and can spontaneously reperfuse. Contrasting this, the proximal filament model was reliable but severe, resulting in a discrepancy in early mortality between treatment groups. These data

emphasize the importance of selecting multiple appropriate models to evaluate potential therapies for ischemic stroke.

In this study, the velocity of blood flow calculated using LSCI is best used as a relative measure within an animal rather than an actual measure of blood flow velocity itself. Using TPLSM as an imaging tool to measure collateral blood flow may be incorporated into future studies to provide a direct measure of red blood cell velocity.

In the filament MCAo study, experiments were not carried out to confirm if the increase in blood flow during TAO were due to blood bypassing the filament rather than an increase in collateral blood flow. This can be verified by carrying out a study using TPLSM to confirm that augmented flow reflects increased flow through ACA-MCA anastomoses. Additionally, the early infarction volume measured after the imaging study did not account for cerebral edema after stroke which might have overestimated the lesion size. Furthermore, functional outcomes after treatment were not measured due to the short time window in the imaging study.

4.6. Future studies

4.6.1. Cortical blood flow changes after TAO in distal MCAo

Our results show that blood flow increases during TAO in a thromboembolic model, with a more variable result in the filament model. Due to the ambiguity of these results, it is necessary to investigate blood flow changes after TAO in a permanent distal MCAo model that will permit evaluation in a permanent, cortical ischemic stroke model of moderate severity and low early mortality.

4.6.2. Two photon imaging of collateral blood vessels with and without TAO

While LSCI maps show relative changes in blood flow, they are susceptible to imaging artefacts and are only semi-quantitative.[112,108] Two photon laser scanning microscopy (TPLSM) permits quantitative measures of blood flow velocity, flux, and vessel diameter above and below the surface and could be used to precisely quantify the blood flow dynamics after TAO.

TPLSM can precisely measure the blood flow in veins, venules, arteries, arterioles and capillaries. It also allows for quantification of direction and velocity of blood cells within the vessels.[37] Since TPLSM can identify capillaries that were not carrying blood before stroke,[118,119] it can strongly

demonstrate the blood flow in anastomoses after stroke and its augmentation by treatment. By using TPLSM imaging for studying changes in collateral dynamics after TAO, we can precisely determine the blood flow velocity and direction of blood flow on the brain surface as well as the vessels in microvascular bed. The three dimensional reconstructions of their microvascular architecture can be obtained along with diameter of vessels.

4.6.3. Long term collateral dynamics after TAO

The studies given above have assessed only the early changes in collateral blood flow after TAO in an ischemic stroke. Therefore, it would be beneficial to know if TAO can maintain collateral perfusion for longer than 24 hours after an ischemic stroke. Armitage et al [46] showed that the collateral vasculature is dynamic and can maintain perfusion of ischemic territories for at least 24 hours after a MCAo.

4.6.4. Combinational therapies with TAO

As mentioned previously, cerebral blood flow augmentation using sphenopalatine ganglion stimulation and head positioning increases blood flow velocity with in the brain by manipulating the neurovascular interface and increasing arterial blood flow due to gravity respectively. [77, 82, 84, 88] The administration of these potential therapies with TAO should be explored. However, the safety of using supine head positioning along with TAO must

be tested, as supine head positioning might increase the intracranial pressure in some patients.[89]

4.7. Conclusions

The experiments presented in this thesis assessed the efficacy of TAO in increasing collateral blood flow in thromboembolic and filament models of MCAo in rats. We demonstrate that TAO dilates the distal branches of MCA during treatment, thereby preventing the collateral collapse in thromboembolic MCAo. The blood flow rate in these distal MCA branches increased during TAO and persists even after the removal of the catheter. A benefit of TAO was not as apparent proximal MCAo by filament occlusion. However, TAO appeared to reduce the MCAo induced mortality in the filament model and some animals exhibited drastic increases in collateral blood flow. The effects of TAO on infarct volume were variable, but suggest a potential neuroprotective effect. One week after thromboembolic MCAo, TAO offers protection to striatum, possibly bymoving the clot past the lenticulostriate arteries. In conclusion, these studies support the contention that TAO can augment collateral blood flow and is most beneficial in patients with moderate stroke, thereby further emphasizing the need for patient selection for evaluating new therapies to treat ischemic stroke.

4.8. Reference

1. Roger VL, Go AS, Lloyd-Jones DM, Benjamin EJ, Berry JD, Borden WB, Bravata DM, Dai S, Ford ES, Fox CS, Fullerton HJ, Gillespie C, Hailpern SM, Heit JA, Howard VJ, Kissela BM, Kittner SJ, Lackland DT, Lichtman JH, Lisabeth LD, Makuc DM, Marcus GM, Marelli A, Matchar DB, Moy CS, Mozaffarian D, Mussolino ME, Nichol G, Paynter NP, Soliman EZ, Sorlie PD, Sotoodehnia N, Turan TN, Virani SS, Wong ND, Woo D, Turner MB. Heart disease and stroke statistics--2012 update: A report from the american heart association. *Circulation*. 2012;125:e2-e220
2. Mukherjee D, Patil CG. Epidemiology and the global burden of stroke. *World neurosurgery*. 2011;76:S85-90
3. Mittmann N, Seung SJ, Hill MD, Phillips SJ, Hachinski V, Cote R, Buck BH, Mackey A, Gladstone DJ, Howse DC, Shuaib A, Sharma M. Impact of disability status on ischemic stroke costs in canada in the first year. *The Canadian journal of neurological sciences. Le journal canadien des sciences neurologiques*. 2012;39:793-800
4. Sacco RL, Wolf PA, Gorelick PB. Risk factors and their management for stroke prevention: Outlook for 1999 and beyond. *Neurology*. 1999;53:S15-24
5. Simons LA, McCallum J, Friedlander Y, Simons J. Risk factors for ischemic stroke: Dubbo study of the elderly. *Stroke; a journal of cerebral circulation*. 1998;29:1341-1346
6. Grysiewicz RA, Thomas K, Pandey DK. Epidemiology of ischemic and hemorrhagic stroke: Incidence, prevalence, mortality, and risk factors. *Neurologic clinics*. 2008;26:871-895, vii
7. Broderick J, Connolly S, Feldmann E, Hanley D, Kase C, Krieger D, Mayberg M, Morgenstern L, Ogilvy CS, Vespa P, Zuccarello M. Guidelines for the management of spontaneous intracerebral hemorrhage in adults: 2007 update: A guideline from the american heart association/american stroke association stroke council, high blood pressure research council, and the quality of care and outcomes in research interdisciplinary working group. *Stroke; a journal of cerebral circulation*. 2007;38:2001-2023
8. Cross DT, 3rd, Tirschwell DL, Clark MA, Tuden D, Derdeyn CP, Moran CJ, Dacey RG, Jr. Mortality rates after subarachnoid hemorrhage: Variations according to hospital case volume in 18 states. *Journal of neurosurgery*. 2003;99:810-817
9. Rosamond W, Flegal K, Furie K, Go A, Greenlund K, Haase N, Hailpern SM, Ho M, Howard V, Kissela B, Kittner S, Lloyd-Jones D, McDermott M, Meigs J, Moy C, Nichol G, O'Donnell C, Roger V, Sorlie P, Steinberger J, Thom T, Wilson M, Hong Y. Heart

disease and stroke statistics--2008 update: A report from the american heart association statistics committee and stroke statistics subcommittee. *Circulation*. 2008;117:e25-146
10. Donnan GA, Fisher M, Macleod M, Davis SM. Stroke. *Lancet*. 2008;371:1612-1623
11. Hossmann KA. Pathophysiology and therapy of experimental stroke. *Cellular and molecular neurobiology*. 2006;26:1057-1083
12. Albers GW, Caplan LR, Easton JD, Fayad PB, Mohr JP, Saver JL, Sherman DG. Transient ischemic attack--proposal for a new definition. *The New England journal of medicine*. 2002;347:1713-1716
13. Dirnagl U, Iadecola C, Moskowitz MA. Pathobiology of ischaemic stroke: An integrated view. *Trends in neurosciences*. 1999;22:391-397
14. Hakim AM. The cerebral ischemic penumbra. *The Canadian journal of neurological sciences. Le journal canadien des sciences neurologiques*. 1987;14:557-559
15. Ginsberg MD. Neuroprotection for ischemic stroke: Past, present and future. *Neuropharmacology*. 2008;55:363-389
16. Wahlgren NG, Ahmed N. Neuroprotection in cerebral ischaemia: Facts and fancies--the need for new approaches. *Cerebrovasc Dis*. 2004;17 Suppl 1:153-166
17. Wardlaw JM, Murray V, Berge E, Del Zoppo GJ. Thrombolysis for acute ischaemic stroke. *The Cochrane database of systematic reviews*. 2009:CD000213
18. Hacke W, Kaste M, Bluhmki E, Brozman M, Davalos A, Guidetti D, Larrue V, Lees KR, Medeghri Z, Machnig T, Schneider D, von Kummer R, Wahlgren N, Toni D. Thrombolysis with alteplase 3 to 4.5 hours after acute ischemic stroke. *The New England journal of medicine*. 2008;359:1317-1329
19. Tissue plasminogen activator for acute ischemic stroke. The national institute of neurological disorders and stroke rt-pa stroke study group. *The New England journal of medicine*. 1995;333:1581-1587
20. Donnan GA, Davis SM, Chambers BR, Gates PC, Hankey GJ, McNeil JJ, Rosen D, Stewart-Wynne EG, Tuck RR. Streptokinase for acute ischemic stroke with relationship to time of administration: Australian streptokinase (ask) trial study group. *JAMA : the journal of the American Medical Association*. 1996;276:961-966
21. Fiorelli M, Bastianello S, von Kummer R, del Zoppo GJ, Larrue V, Lesaffre E, Ringleb AP, Lorenzano S, Manelfe C, Bozzao L. Hemorrhagic transformation within 36 hours of a cerebral infarct: Relationships with early clinical deterioration and 3-month outcome

in the european cooperative acute stroke study i (ecass i) cohort. *Stroke; a journal of cerebral circulation*. 1999;30:2280-2284
22. Kwan J, Hand P, Sandercock P. A systematic review of barriers to delivery of thrombolysis for acute stroke. *Age and ageing*. 2004;33:116-121
23. Fang MC, Cutler DM, Rosen AB. Trends in thrombolytic use for ischemic stroke in the united states. *Journal of hospital medicine : an official publication of the Society of Hospital Medicine*. 2010;5:406-409
24. Saqqur M, Uchino K, Demchuk AM, Molina CA, Garami Z, Calleja S, Akhtar N, Orouk FO, Salam A, Shuaib A, Alexandrov AV. Site of arterial occlusion identified by transcranial doppler predicts the response to intravenous thrombolysis for stroke. *Stroke; a journal of cerebral circulation*. 2007;38:948-954
25. del Zoppo GJ, Poeck K, Pessin MS, Wolpert SM, Furlan AJ, Ferbert A, Alberts MJ, Zivin JA, Wechsler L, Busse O, et al. Recombinant tissue plasminogen activator in acute thrombotic and embolic stroke. *Annals of neurology*. 1992;32:78-86
26. Liebeskind DS. Collateral circulation. *Stroke; a journal of cerebral circulation*. 2003;34:2279-2284
27. Hendrikse J, van Raamt AF, van der Graaf Y, Mali WP, van der Grond J. Distribution of cerebral blood flow in the circle of willis. *Radiology*. 2005;235:184-189
28. Cieslicki K, Gielecki J, Wilczak T. [redundancy of the main cerebral arteries in morphological variations of the willis circle]. *Neurologia i neurochirurgia polska*. 1997;31:463-474
29. Kolb B, Whishaw IQ. *Fundamentals of human neuropsychology*. New York, United States: W.H. Freeman; 1996.
30. Cipolla MJ. *The cerebral circulation*. San Rafael (CA); 2009.
31. Henderson RD, Eliasziw M, Fox AJ, Rothwell PM, Barnett HJ. Angiographically defined collateral circulation and risk of stroke in patients with severe carotid artery stenosis. North american symptomatic carotid endarterectomy trial (nascet) group. *Stroke; a journal of cerebral circulation*. 2000;31:128-132
32. Reynolds PS, Greenberg JP, Lien LM, Meads DC, Myers LG, Tegeler CH. Ophthalmic artery flow direction on color flow duplex imaging is highly specific for severe carotid stenosis. *Journal of neuroimaging : official journal of the American Society of Neuroimaging*. 2002;12:5-8
33. Liebeskind DS. Collaterals in acute stroke: Beyond the clot. *Neuroimaging clinics of North America*. 2005;15:553-573, x
34. Angermaier A, Langner S, Kirsch M, Kessler C, Hosten N, Khaw AV. Ct-angiographic collateralization predicts final infarct volume

after intra-arterial thrombolysis for acute anterior circulation ischemic stroke. *Cerebrovasc Dis*. 2011;31:177-184
35. Bang OY, Saver JL, Buck BH, Alger JR, Starkman S, Ovbiagele B, Kim D, Jahan R, Duckwiler GR, Yoon SR, Vinuela F, Liebeskind DS. Impact of collateral flow on tissue fate in acute ischaemic stroke. *Journal of neurology, neurosurgery, and psychiatry*. 2008;79:625-629
36. Zhang H, Prabhakar P, Sealock R, Faber JE. Wide genetic variation in the native pial collateral circulation is a major determinant of variation in severity of stroke. *Journal of cerebral blood flow and metabolism : official journal of the International Society of Cerebral Blood Flow and Metabolism*. 2010;30:923-934
37. Ramakrishnan G, Armitage GA, Winship IR. Understanding and augmenting collateral blood flow during ischemic stroke. *Acute Ischemic Stroke*. 2012:25
38. Hartung MP, Grist TM, Francois CJ. Magnetic resonance angiography: Current status and future directions. *Journal of cardiovascular magnetic resonance : official journal of the Society for Cardiovascular Magnetic Resonance*. 2011;13:19
39. Furst G, Steinmetz H, Fischer H, Skutta B, Sitzer M, Aulich A, Kahn T, Modder U. Selective mr angiography and intracranial collateral blood flow. *Journal of computer assisted tomography*. 1993;17:178-183
40. Barlinn K, Alexandrov AV. Vascular imaging in stroke: Comparative analysis. *Neurotherapeutics : the journal of the American Society for Experimental NeuroTherapeutics*. 2011;8:340-348
41. Schellinger PD. The evolving role of advanced mr imaging as a management tool for adult ischemic stroke: A western-european perspective. *Neuroimaging clinics of North America*. 2005;15:245-258, ix
42. Zhang S, Boyd J, Delaney K, Murphy TH. Rapid reversible changes in dendritic spine structure in vivo gated by the degree of ischemia. *The Journal of neuroscience : the official journal of the Society for Neuroscience*. 2005;25:5333-5338
43. Zhang S, Murphy TH. Imaging the impact of cortical microcirculation on synaptic structure and sensory-evoked hemodynamic responses in vivo. *PLoS biology*. 2007;5:e119
44. Winship IR, Murphy TH. In vivo calcium imaging reveals functional rewiring of single somatosensory neurons after stroke. *The Journal of neuroscience : the official journal of the Society for Neuroscience*. 2008;28:6592-6606

45. Winship IR, Murphy TH. Remapping the somatosensory cortex after stroke: Insight from imaging the synapse to network. *The Neuroscientist : a review journal bringing neurobiology, neurology and psychiatry*. 2009;15:507-524
46. Armitage GA, Todd KG, Shuaib A, Winship IR. Laser speckle contrast imaging of collateral blood flow during acute ischemic stroke. *Journal of cerebral blood flow and metabolism : official journal of the International Society of Cerebral Blood Flow and Metabolism*. 2010;30:1432-1436
47. Brozici M, van der Zwan A, Hillen B. Anatomy and functionality of leptomeningeal anastomoses: A review. *Stroke; a journal of cerebral circulation*. 2003;34:2750-2762
48. Choi S, Lee MG, Park JK. Microfluidic parallel circuit for measurement of hydraulic resistance. *Biomicrofluidics*. 2010;4
49. Christoforidis GA, Mohammad Y, Kehagias D, Avutu B, Slivka AP. Angiographic assessment of pial collaterals as a prognostic indicator following intra-arterial thrombolysis for acute ischemic stroke. *AJNR. American journal of neuroradiology*. 2005;26:1789-1797
50. Miteff F, Levi CR, Bateman GA, Spratt N, McElduff P, Parsons MW. The independent predictive utility of computed tomography angiographic collateral status in acute ischaemic stroke. *Brain : a journal of neurology*. 2009;132:2231-2238
51. Lima FO, Furie KL, Silva GS, Lev MH, Camargo EC, Singhal AB, Harris GJ, Halpern EF, Koroshetz WJ, Smith WS, Yoo AJ, Nogueira RG. The pattern of leptomeningeal collaterals on ct angiography is a strong predictor of long-term functional outcome in stroke patients with large vessel intracranial occlusion. *Stroke; a journal of cerebral circulation*. 2010;41:2316-2322
52. Robertson RL, Burrows PE, Barnes PD, Robson CD, Poussaint TY, Scott RM. Angiographic changes after pial synangiosis in childhood moyamoya disease. *AJNR. American journal of neuroradiology*. 1997;18:837-845
53. Mori N, Mugikura S, Higano S, Kaneta T, Fujimura M, Umetsu A, Murata T, Takahashi S. The leptomeningeal "ivy sign" on fluid-attenuated inversion recovery mr imaging in moyamoya disease: A sign of decreased cerebral vascular reserve? *AJNR. American journal of neuroradiology*. 2009;30:930-935
54. Chung PW, Park KY. Leptomeningeal enhancement in petients with moyamoya disease: Correlation with perfusion imaging. *Neurology*. 2009;72:1872-1873
55. Yamauchi H, Kudoh T, Sugimoto K, Takahashi M, Kishibe Y, Okazawa H. Pattern of collaterals, type of infarcts, and

haemodynamic impairment in carotid artery occlusion. *Journal of neurology, neurosurgery, and psychiatry*. 2004;75:1697-1701
56. Bang OY, Saver JL, Kim SJ, Kim GM, Chung CS, Ovbiagele B, Lee KH, Liebeskind DS. Collateral flow predicts response to endovascular therapy for acute ischemic stroke. *Stroke; a journal of cerebral circulation*. 2011;42:693-699
57. Chalothorn D, Clayton JA, Zhang H, Pomp D, Faber JE. Collateral density, remodeling, and vegf-a expression differ widely between mouse strains. *Physiological genomics*. 2007;30:179-191
58. Menzies SA, Hoff JT, Betz AL. Middle cerebral artery occlusion in rats: A neurological and pathological evaluation of a reproducible model. *Neurosurgery*. 1992;31:100-106; discussion 106-107
59. Morita Y, Fukuuchi Y, Koto A, Suzuki N, Isozumi K, Gotoh J, Shimizu T, Takao M, Aoyama M. Rapid changes in pial arterial diameter and cerebral blood flow caused by ipsilateral carotid artery occlusion in rats. *The Keio journal of medicine*. 1997;46:120-127
60. Shima T, Hossmann KA, Date H. Pial arterial pressure in cats following middle cerebral artery occlusion. 1. Relationship to blood flow, regulation of blood flow and electrophysiological function. *Stroke; a journal of cerebral circulation*. 1983;14:713-719
61. Derdeyn CP, Powers WJ, Grubb RL, Jr. Hemodynamic effects of middle cerebral artery stenosis and occlusion. *AJNR. American journal of neuroradiology*. 1998;19:1463-1469
62. Coyle P, Heistad DD. Blood flow through cerebral collateral vessels one month after middle cerebral artery occlusion. *Stroke; a journal of cerebral circulation*. 1987;18:407-411
63. Schirmer SH, van Nooijen FC, Piek JJ, van Royen N. Stimulation of collateral artery growth: Travelling further down the road to clinical application. *Heart*. 2009;95:191-197
64. Deb P, Sharma S, Hassan KM. Pathophysiologic mechanisms of acute ischemic stroke: An overview with emphasis on therapeutic significance beyond thrombolysis. *Pathophysiology : the official journal of the International Society for Pathophysiology / ISP*. 2010;17:197-218
65. Sun Y, Jin K, Xie L, Childs J, Mao XO, Logvinova A, Greenberg DA. Vegf-induced neuroprotection, neurogenesis, and angiogenesis after focal cerebral ischemia. *The Journal of clinical investigation*. 2003;111:1843-1851
66. Zhang ZG, Zhang L, Jiang Q, Zhang R, Davies K, Powers C, Bruggen N, Chopp M. Vegf enhances angiogenesis and promotes blood-brain barrier leakage in the ischemic brain. *The Journal of clinical investigation*. 2000;106:829-838

67. Weis SM, Cheresh DA. Pathophysiological consequences of vegf-induced vascular permeability. *Nature*. 2005;437:497-504
68. Manoonkitiwongsa PS, Schultz RL, McCreery DB, Whitter EF, Lyden PD. Neuroprotection of ischemic brain by vascular endothelial growth factor is critically dependent on proper dosage and may be compromised by angiogenesis. *Journal of cerebral blood flow and metabolism : official journal of the International Society of Cerebral Blood Flow and Metabolism*. 2004;24:693-702
69. Navaratna D, Guo S, Arai K, Lo EH. Mechanisms and targets for angiogenic therapy after stroke. *Cell adhesion & migration*. 2009;3:216-223
70. Pyun WB, Hahn W, Kim DS, Yoo WS, Lee SD, Won JH, Rho BS, Park ZY, Kim JM, Kim S. Naked DNA expressing two isoforms of hepatocyte growth factor induces collateral artery augmentation in a rabbit model of limb ischemia. *Gene therapy*. 2010;17:1442-1452
71. Todo K, Kitagawa K, Sasaki T, Omura-Matsuoka E, Terasaki Y, Oyama N, Yagita Y, Hori M. Granulocyte-macrophage colony-stimulating factor enhances leptomeningeal collateral growth induced by common carotid artery occlusion. *Stroke; a journal of cerebral circulation*. 2008;39:1875-1882
72. Nakagawa T, Suga S, Kawase T, Toda M. Intracarotid injection of granulocyte-macrophage colony-stimulating factor induces neuroprotection in a rat transient middle cerebral artery occlusion model. *Brain research*. 2006;1089:179-185
73. Schabitz WR, Kruger C, Pitzer C, Weber D, Laage R, Gassler N, Aronowski J, Mier W, Kirsch F, Dittgen T, Bach A, Sommer C, Schneider A. A neuroprotective function for the hematopoietic protein granulocyte-macrophage colony stimulating factor (gm-csf). *Journal of cerebral blood flow and metabolism : official journal of the International Society of Cerebral Blood Flow and Metabolism*. 2008;28:29-43
74. Sugiyama Y, Yagita Y, Oyama N, Terasaki Y, Omura-Matsuoka E, Sasaki T, Kitagawa K. Granulocyte colony-stimulating factor enhances arteriogenesis and ameliorates cerebral damage in a mouse model of ischemic stroke. *Stroke; a journal of cerebral circulation*. 2011;42:770-775
75. Wityk RJ. Blood pressure augmentation in acute ischemic stroke. *Journal of the neurological sciences*. 2007;261:63-73
76. Bogoslovsky T, Happola O, Salonen O, Lindsberg PJ. Induced hypertension for the treatment of acute mca occlusion beyond the thrombolysis window: Case report. *BMC neurology*. 2006;6:46
77. Shin HK, Nishimura M, Jones PB, Ay H, Boas DA, Moskowitz MA, Ayata C. Mild induced hypertension improves blood flow and

oxygen metabolism in transient focal cerebral ischemia. *Stroke; a journal of cerebral circulation*. 2008;39:1548-1555
78. Smrcka M, Ogilvy CS, Crow RJ, Maynard KI, Kawamata T, Ames A, 3rd. Induced hypertension improves regional blood flow and protects against infarction during focal ischemia: Time course of changes in blood flow measured by laser doppler imaging. *Neurosurgery*. 1998;42:617-624; discussion 624-615
79. Chileuitt L, Leber K, McCalden T, Weinstein PR. Induced hypertension during ischemia reduces infarct area after temporary middle cerebral artery occlusion in rats. *Surgical neurology*. 1996;46:229-234
80. Hillis AE, Ulatowski JA, Barker PB, Torbey M, Ziai W, Beauchamp NJ, Oh S, Wityk RJ. A pilot randomized trial of induced blood pressure elevation: Effects on function and focal perfusion in acute and subacute stroke. *Cerebrovasc Dis*. 2003;16:236-246
81. Rordorf G, Koroshetz WJ, Ezzeddine MA, Segal AZ, Buonanno FS. A pilot study of drug-induced hypertension for treatment of acute stroke. *Neurology*. 2001;56:1210-1213
82. Ayajiki K, Fujioka H, Shinozaki K, Okamura T. Effects of capsaicin and nitric oxide synthase inhibitor on increase in cerebral blood flow induced by sensory and parasympathetic nerve stimulation in the rat. *J Appl Physiol*. 2005;98:1792-1798
83. Suzuki N, Hardebo JE, Kahrstrom J, Owman C. Selective electrical stimulation of postganglionic cerebrovascular parasympathetic nerve fibers originating from the sphenopalatine ganglion enhances cortical blood flow in the rat. *Journal of cerebral blood flow and metabolism : official journal of the International Society of Cerebral Blood Flow and Metabolism*. 1990;10:383-391
84. Yarnitsky D, Lorian A, Shalev A, Zhang ZD, Takahashi M, Agbaje-Williams M, Macdonald RL. Reversal of cerebral vasospasm by sphenopalatine ganglion stimulation in a dog model of subarachnoid hemorrhage. *Surgical neurology*. 2005;64:5-11; discussion 11
85. Levi H, Schoknecht K, Prager O, Chassidim Y, Weissberg I, Serlin Y, Friedman A. Stimulation of the sphenopalatine ganglion induces reperfusion and blood-brain barrier protection in the photothrombotic stroke model. *PloS one*. 2012;7:e39636
86. Bar-Shir A, Shemesh N, Nossin-Manor R, Cohen Y. Late stimulation of the sphenopalatine-ganglion in ischemic rats: Improvement in n-acetyl-aspartate levels and diffusion weighted imaging characteristics as seen by mr. *Journal of magnetic resonance imaging : JMRI*. 2010;31:1355-1363
87. Khurana D, Kaul S, Bornstein NM. Implant for augmentation of cerebral blood flow trial 1: A pilot study evaluating the safety and

effectiveness of the ischaemic stroke system for treatment of acute ischaemic stroke. *International journal of stroke : official journal of the International Stroke Society*. 2009;4:480-485
88. Wojner-Alexander AW, Garami Z, Chernyshev OY, Alexandrov AV. Heads down: Flat positioning improves blood flow velocity in acute ischemic stroke. *Neurology*. 2005;64:1354-1357
89. Schwarz S, Georgiadis D, Aschoff A, Schwab S. Effects of induced hypertension on intracranial pressure and flow velocities of the middle cerebral arteries in patients with large hemispheric stroke. *Stroke; a journal of cerebral circulation*. 2002;33:998-1004
90. Moraine JJ, Berre J, Melot C. Is cerebral perfusion pressure a major determinant of cerebral blood flow during head elevation in comatose patients with severe intracranial lesions? *Journal of neurosurgery*. 2000;92:606-614
91. Lylyk P, Vila JF, Miranda C, Ferrario A, Romero R, Cohen JE. Partial aortic obstruction improves cerebral perfusion and clinical symptoms in patients with symptomatic vasospasm. *Neurological research*. 2005;27 Suppl 1:S129-135
92. Hammer M, Jovin T, Wahr JA, Heiss WD. Partial occlusion of the descending aorta increases cerebral blood flow in a nonstroke porcine model. *Cerebrovasc Dis*. 2009;28:406-410
93. Noor R, Wang CX, Todd K, Elliott C, Wahr J, Shuaib A. Partial intra-aortic occlusion improves perfusion deficits and infarct size following focal cerebral ischemia. *Journal of neuroimaging : official journal of the American Society of Neuroimaging*. 2010;20:272-276
94. Gerrits RJ, Stein EA, Greene AS. Laser-doppler flowmetry utilizing a thinned skull cranial window preparation and automated stimulation. *Brain research. Brain research protocols*. 1998;3:14-21
95. Armitage GA. *Dynamics of the collateral vascular system [dissertation]*. Ann Arbor: University of Alberta (Canada); 2010.
96. Winship IR, Armitage GA, Ramakrishnan G, Dong B, Todd KG, Shuaib A. Augmenting collateral blood flow during ischemic stroke via transient aortic occlusion. *Journal of cerebral blood flow and metabolism : official journal of the International Society of Cerebral Blood Flow and Metabolism*. 2013
97. Duncan DD, Kirkpatrick SJ. Can laser speckle flowmetry be made a quantitative tool? *Journal of the Optical Society of America. A, Optics, image science, and vision*. 2008;25:2088-2094
98. Shuaib A, Bornstein NM, Diener HC, Dillon W, Fisher M, Hammer MD, Molina CA, Rutledge JN, Saver JL, Schellinger PD, Shownkeen H. Partial aortic occlusion for cerebral perfusion augmentation: Safety and efficacy of neuroflo in acute ischemic

stroke trial. *Stroke; a journal of cerebral circulation*. 2011;42:1680-1690
99. Shuaib A, Butcher K, Mohammad AA, Saqqur M, Liebeskind DS. Collateral blood vessels in acute ischaemic stroke: A potential therapeutic target. *Lancet neurology*. 2011;10:909-921
100. Emery DJ, Schellinger PD, Selchen D, Douen AG, Chan R, Shuaib A, Butcher KS. Safety and feasibility of collateral blood flow augmentation after intravenous thrombolysis. *Stroke; a journal of cerebral circulation*. 2011;42:1135-1137
101. Saqqur M, Ibrahim M, Butcher K, Khan K, Emery D, Manawadu D, Derksen C, Schwindt B, Shuaib A. Transcranial doppler and cerebral augmentation in acute ischemic stroke. *Journal of neuroimaging : official journal of the American Society of Neuroimaging*. 2013;23:460-465
102. Paxinos G, Watson C. *The rat brain in stereotaxic coordinates*. San Diego: Academic press; 2007.
103. Carmichael ST. Rodent models of focal stroke: Size, mechanism, and purpose. *NeuroRx : the journal of the American Society for Experimental NeuroTherapeutics*. 2005;2:396-409
104. Wang CX, Yang Y, Yang T, Shuaib A. A focal embolic model of cerebral ischemia in rats: Introduction and evaluation. *Brain research. Brain research protocols*. 2001;7:115-120
105. Li Y, Zhu S, Yuan L, Lu H, Li H, Tong S. Predicting the ischemic infarct volume at the first minute after occlusion in rodent stroke model by laser speckle imaging of cerebral blood flow. *Journal of biomedical optics*. 2013;18:76024
106. Dunn AK, Bolay H, Moskowitz MA, Boas DA. Dynamic imaging of cerebral blood flow using laser speckle. *Journal of cerebral blood flow and metabolism : official journal of the International Society of Cerebral Blood Flow and Metabolism*. 2001;21:195-201
107. Strong AJ, Bezzina EL, Anderson PJ, Boutelle MG, Hopwood SE, Dunn AK. Evaluation of laser speckle flowmetry for imaging cortical perfusion in experimental stroke studies: Quantitation of perfusion and detection of peri-infarct depolarisations. *Journal of cerebral blood flow and metabolism : official journal of the International Society of Cerebral Blood Flow and Metabolism*. 2006;26:645-653
108. Ayata C, Dunn AK, Gursoy OY, Huang Z, Boas DA, Moskowitz MA. Laser speckle flowmetry for the study of cerebrovascular physiology in normal and ischemic mouse cortex. *Journal of cerebral blood flow and metabolism : official journal of the International Society of Cerebral Blood Flow and Metabolism*. 2004;24:744-755

109. Dunn AK. Laser speckle contrast imaging of cerebral blood flow. *Annals of biomedical engineering*. 2012;40:367-377
110. Fischer MJ, Uchida S, Messlinger K. Measurement of meningeal blood vessel diameter in vivo with a plug-in for imagej. *Microvascular research*. 2010;80:258-266
111. Stokland O, Thorvaldson J, Ilebekk A, Kiil F. Contributions of blood drainage from the liver, spleen and intestines to cardiac effects of aortic occlusion in the dog. *Acta physiologica Scandinavica*. 1982;114:351-362
112. Parthasarathy AB, Tom WJ, Gopal A, Zhang X, Dunn AK. Robust flow measurement with multi-exposure speckle imaging. *Optics express*. 2008;16:1975-1989
113. Li P, Ni S, Zhang L, Zeng S, Luo Q. Imaging cerebral blood flow through the intact rat skull with temporal laser speckle imaging. *Optics letters*. 2006;31:1824-1826
114. Gonzalez NR, Hamilton R, Bilgin-Freiert A, Dusick J, Vespa P, Hu X, Asgari S. Cerebral hemodynamic and metabolic effects of remote ischemic preconditioning in patients with subarachnoid hemorrhage. *Acta neurochirurgica. Supplement*. 2013;115:193-198
115. Shuaib A, Schwab S, Rutledge JN, Starkman S, Liebeskind DS, Bernardini GL, Boulos A, Abou-Chebl A, Huang DY, Vanhooren G, Cruz-Flores S, Klucznik RP, Saver JL. Importance of proper patient selection and endpoint selection in evaluation of new therapies in acute stroke: Further analysis of the sentis trial. *Journal of neurointerventional surgery*. 2013;5 Suppl 1:i21-24
116. O'Collins VE, Macleod MR, Donnan GA, Horky LL, van der Worp BH, Howells DW. 1,026 experimental treatments in acute stroke. *Annals of neurology*. 2006;59:467-477
117. Recommendations for standards regarding preclinical neuroprotective and restorative drug development. *Stroke; a journal of cerebral circulation*. 1999;30:2752-2758
118. Schaffer CB, Friedman B, Nishimura N, Schroeder LF, Tsai PS, Ebner FF, Lyden PD, Kleinfeld D. Two-photon imaging of cortical surface microvessels reveals a robust redistribution in blood flow after vascular occlusion. *PLoS biology*. 2006;4:e22
119. Shih AY, Friedman B, Drew PJ, Tsai PS, Lyden PD, Kleinfeld D. Active dilation of penetrating arterioles restores red blood cell flux to penumbral neocortex after focal stroke. *Journal of cerebral blood flow and metabolism : official journal of the International Society of Cerebral Blood Flow and Metabolism*. 2009;29:738-751